

UNCLASSIFIED

AD NUMBER
AD823704
NEW LIMITATION CHANGE
TO Approved for public release, distribution unlimited
FROM Distribution authorized to U.S. Gov't. agencies only; Test and Evaluation; DEC 1971. Other requests shall be referred to Air Force Flight Dynamics Laboratory, Attn: FY, Wright-Patterson AFB, OH 45433.
AUTHORITY
AFML ltr dtd 12 Jan 1972

THIS PAGE IS UNCLASSIFIED

DEVELOPMENT OF A TUNED DAMPER TO REDUCE VIBRATION DAMAGE IN AN AIRCRAFT RADAR ANTENNA

D. I. G. JONES, A. D. NASHIF, 1/LT G. H. BRUNS,
R. SEVY, F. S. OWENS, J. P. HENDERSON, and R. L. CONNER

TECHNICAL REPORT No. AFML-TR-67-307

SEPTEMBER 1967

Distribution limited to U. S. Government agencies only;
test and evaluation; statement applied Dec 71
Other requests for this document must be referred to AF Flight
Dynamics Laboratory, (FY), Wright-Patterson AFB, Ohio 45433.

AIR FORCE MATERIALS LABORATORY
RESEARCH AND TECHNOLOGY DIVISION
AIR FORCE SYSTEMS COMMAND
WRIGHT-PATTERSON AIR FORCE BASE, OHIO



Best Available Copy

20070919136

NOTICE

When Government drawings, specifications, or other data are used for any purpose other than in connection with a definitely related Government procurement operation, the United States Government thereby incurs no responsibility nor any obligation whatsoever; and the fact that the Government may have formulated, furnished, or in any way supplied the said drawings, specifications, or other data, is not to be regarded by implication or otherwise as in any manner licensing the holder or any other person or corporation, or conveying any rights or permission to manufacture, use, or sell any patented invention that may in any way be related thereto.

Copies of this report should not be returned unless return is required by security considerations, contractual obligations, or notice on a specific document.

DEVELOPMENT OF A TUNED DAMPER TO REDUCE VIBRATION DAMAGE IN AN AIRCRAFT RADAR ANTENNA

*D. I. G. JONES, A. D. NASHIF, 1/LT G. H. BRUNS,
R. SEVY, F. S. OWENS, J. P. HENDERSON, and R. L. CONNER*

**Distribution limited to U. S. Government agencies only;
test and evaluation; statement applied** Dec 71
Other requests for this document must be referred to AF Flight
Dynamics Laboratory, (FY), Wright-Patterson AFB, Ohio 45433

FOREWORD

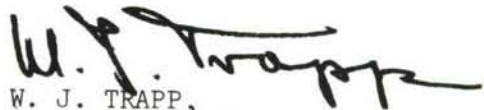
This report was prepared by the Strength and Dynamics Branch, Metals and Ceramics Division, under Project No. 7351, "Metallic Materials", Task No. 735106, "Behavior of Metals". The principal investigation was carried out at the Air Force Materials Laboratory in cooperation with the Air Force Flight Dynamics Laboratory and the University of Dayton under USAF Contract No. AF 33(615)-1506, by Dr. D.I.G. Jones, J.P. Henderson and 1/Lt G.H. Bruns of the Strength and Dynamics Branch; F.S. Owens of the Elastomers and Coatings Branch (MANE); A.D. Nashif (visiting scientist to AFML) and R.L. Conner of the University of Dayton and R. Sevy of the Air Force Flight Dynamics Laboratory. Test equipment purchased using the Directors Fund of the Air Force Materials Laboratory was used in this investigation.

This report covers work performed from January 1966 to May 1967.

The authors wish to thank Mr. W.J. Trapp and Mr. R.E. Headrick for their support, Mr. E. E. Ruddell for assistance with identification of the antenna failure mode, Mr. C. E. Thomas and Mrs. P. Bolds for assistance with synthesis of the vibration spectrum, Mr. J. Schmermund for assistance with the test equipment setup, Mr. E. D. Goens for assistance with the sinusoidal testing, Mr. D. Krintzline for assistance with the molding, Mr. C. M. Cannon for assistance with measuring the viscoelastic material properties, Mr. K. Holdcraft and Mr. D. Devers for assistance with machining the metal parts of the dampers.

The manuscript was released by the authors May 1967 for publication.

This technical report has been reviewed and is approved.



W. J. TRAPP,
Chief, Strength and Dynamics Branch
Metals and Ceramics Division
Air Force Materials Laboratory

ABSTRACT

The application of the facilities and expertise of several research and development laboratories at Wright-Patterson Air Force Base, as well as other organizations, to the solution of a critical Air Force vibration problem is described in this technical report. Specifically, the development of a tuned damper to increase the service life of an aircraft radar antenna suffering from severe vibration damage is described. The resulting tuned damper was a wide temperature range device capable of operating satisfactorily in a severe vibrational environment. Criteria necessary for the development of wider temperature range dampers were established in the course of the investigation.

This abstract is subject to special export controls and each transmittal to foreign governments and foreign nationals may be made only with the prior approval of the Metals and Ceramics Division, MAM, Air Force Materials Laboratory, Wright-Patterson Air Force Base, Ohio 45433.

TABLE OF CONTENTS

	PAGE
I. INTRODUCTION	1
II. THE SERVICE ENVIRONMENT AND ITS SIMULATION	3
III. THE VIBRATION PROBLEM AND POSSIBLE SOLUTIONS	9
IV. INITIAL DAMPER DESIGNS AND THEIR TESTING	11
V. PROTOTYPE AND PRODUCTION DAMPER DESIGNS USING NITRILE RUBBERS	13
VI. FIELD TESTS	19
VII. CONCLUSIONS	20
REFERENCES	21
TABLE	22

ILLUSTRATIONS

FIGURE		PAGE
1.	Longitudinal Spatial Relationships of Vibration Pickup and Antenna	23
2.	Relative Locations of Cannon, Pickups and Antenna . . .	24
3.	Probability Density Distribution of F-100 Gunfire Record	25
4.	Derived Broad-Band Random Spectrum	26
5.	Schematic of Radar Antenna	27
6.	Photograph of Antenna	28
7.	Typical Response Spectra for Undamped Antenna	29
8.	Failure in Antenna	30
9.	Damping Properties of VPCO-15080 [7]	31
10.	Prototype I Damper Geometry	32
11.	Location of Damper on Connector	33
12.	Typical Response Spectra for Antenna with and without Prototype Damper	34
13.	Variation of Amplification Factor A with Temperature for Antenna with Prototype I Attached. . . .	35
14.	Damping Properties of Paracril-D	36
15.	Geometry of Prototype 2	37
16.	Variation of Amplification Factor A with Temperature for Antenna with Prototypes 2 and 3 Attached	38
17.	Exploded View of Mold	39
18.	Layout of Damper in Mold	40
19.	Geometry of Prototype 2	41
20.	Variation of Amplification Factor A with Temperature for Antenna with Prototype 4 Attached (1 and 5-g input)	42

ILLUSTRATIONS (CONT'D)

FIGURE		PAGE
21.	Variation of Amplification Factor A with Temperature for Antenna with Prototype 4 Attached (10 and 20-g input)	43
22.	Damping Properties of Paracril-BJ	44
23.	Variation of Amplification Factor A with Temperature for Antenna with Prototype 5 Attached	45
24.	Damping Properties of Paracril-BJ with 50 PHR Carbon . .	46
25.	Variation of Amplification Factor A with Temperature for Antenna with Prototype 6 Attached . . .	47
26.	Variation of Amplification Factor A with Temperature for Antenna with Prototype 7 Attached . . .	48
27.	Damping Properties of Paracril-BJ with 25 PHR Carbon . .	49
28.	Geometry of Prototype 8 and Subsequent Dampers	50
29.	Production Damper	51
30.	Production Damper Attached to Antenna	52
31.	Production Damper Attached to Antenna	53
32.	Graphs of Amplification Factor A Against Temperature for Antenna with Prototype 8 Attached . . .	54
33.	Graphs of Amplification Factor A Against Temperature for Antenna with Production Dampers Attached	55
34.	Graphs of Amplification Factor A Against Temperature for Antenna with Production Dampers Attached	56
35.	Graphs of Amplification Factor A Against Temperature for Antenna with TD-11, 12, 13, 15 and 17 Attached	57
36.	Graph of Amplification Factor A Against Life of Antenna	58

SYMBOLS

A	Amplification factor at resonance
B	Spectral analyzer bandwidth
e	Normalized standard error for mean square value estimate
E	Real part of Young's Modulus of viscoelastic material (psi)
f	Frequency (cps)
f_1	Antenna natural frequency (cps)
f_c	See Reference [1]
g	Acceleration due to gravity (ft/sec ²)
K	T/2
m	Tuning mass of damper (gm)
n	Degrees of freedom
$\hat{p}(x)$	Probability density of acceleration sample
T	Averaging time
T	Tape sample length
\bar{V}_o	See Reference [1]
W	Analyzer window
η	Loss factor (or loss tangent) of viscoelastic material

I. INTRODUCTION

This technical report describes the application of the facilities and expertise of several Research and Development Laboratories and Divisions at Wright-Patterson Air Force Base to the solution of a critical Air Force vibration problem. A brief historical review of the highlights of the resulting program is included to give an overview of the effort and to place the contributions of the various organizations in perspective.

The field problem involved low cycle fatigue failure of an aircraft IFF radar antenna. The failure was caused by airframe vibrations induced by gunfire in the neighborhood of the antenna. The problem was brought to the attention of the Air Force Flight Dynamics Laboratory (FDFE), early in 1966, and they were able to simulate with some accuracy the operational gunfire induced environment, using a random shaker system. This development is described in Chapter I in some detail. Under this simulated environment, sample radar antennae displayed the same mode of failure, and about the same time to failure, as in the field. Tests on this facility also revealed that various attempts by the manufacturer to eliminate the problem by stiffening the antenna (see Chapter III) produced no improvement in fatigue life, because of the wide range of frequencies over which significant excitation occurred.

Since the Strength and Dynamics Branch (MAMD) of the Air Force Materials Laboratory (AFML) had a well established in-house program of investigation of the effect of various damping techniques on the vibrational response of complex aerospace structures, and in view of the apparent urgency of the matter FDFE contacted MAMD in February 1966 to determine whether AFML had any suggestions which might lead to a solution. A small task force was therefore assembled within MAMD to seek a solution to the problem as quickly as possible. The development of the initial damper configuration is described in Chapter IV and will not be discussed further here. Suffice it to say that a specific damper configuration utilizing a commercially available viscoelastic material (VPCO-15080, manufactured by Farbwerke Hoechst AG, Frankfurt, Germany) had been developed by early March 1966 and was tested in conjunction with a sample antenna first with sinusoidal excitation and finally with a random vibration spectrum to more accurately simulate the gunfire vibration field. Tests indicated that the life of the antenna was increased by a factor of about 5 compared with that for previously tested undamped antennae. This was very promising, but further testing was held up because of both a lack of antennae and an apparent waning of interest in the problem.

However, following MAMD initiated enquiries in August 1966, it became clear that the dampers were still urgently needed and the task force was promptly reconvened to complete the development of the damper on a top priority basis. It had now become clear that any damper design, to be produced in any substantial quantities, would have to satisfy the following requirements: (i) reproducible damping characteristics (ii) good bonding and (iii) adequate strength to withstand the operational environment in all respects.

The development program is described in Chapter V. As a result of previous measurements of viscoelastic material properties on the MAMD damping material measurement facility, sufficient quantities of reliable damping and stiffness data were available in early September 1966 for a rational material choice to be made. By mid September 1966, after several configuration and material changes, a prototype damper had been made, using a nitrile rubber selected by MAMD and supplied by MANE, which was effective in reducing vibration over a far wider temperature range than the original VPCO-15080 damper. On the basis of tests on this prototype, a mold was designed and machined out of stainless steel.

By the end of September 1966, dampers were being produced with the mold and tested both sinusoidally by MAMD and on the random shaker at FDFE using radar antenna which had been received from the manufacturer earlier in the month. After some initial failures, described in Chapter V, MANE was able to produce damping material with sufficient strength to withstand the operational environment without difficulty. Five dampers were then molded, tested under sinusoidal excitation and sent for field testing in October 1966. Field test data, received in January 1967, indicated that the life of the radar antenna on the aircraft had been increased by a factor of more than four and the antenna replacement interval increased from a few days to at least a month. Further dampers were made for field use.

II. THE SERVICE ENVIRONMENT AND ITS SIMULATION

A. LOCATION OF ANTENNAE

The antenna is located on the underside of the aircraft. Flush mounted and bolted to the skin, it is situated between the barrels of the two upper and lower cannons.

The four cannons are hard mounted. An examination of the available vibration records disclosed three vibration pickups located on the main structure (bulkhead) adjacent to the forward gun mount and near the gun blast shield as shown in Figures 1 and 2. The velocity pickups were of the MB-124 type, triaxially mounted on a milled aluminum block. Pickup orientation was in the standard vertical, lateral and longitudinal directions, referenced to the aircraft axes.

The three pickups represented the most proximate location to the antenna and recorded, essentially, the vibration response of the local structure to gun recoil.

B. SPECTRAL ANALYSIS

Two flight records were selected and analyzed on a Minneapolis-Honeywell Model 9050 analyzer. The half-power bandwidths were 10 and 30 cps over the frequency ranges of 10 to 300 cps and 300 to 1000 cps respectively. The analysis frequency range was between 10 cps and 1000 cps. This gross look provided means by which the best data (unclipped) and the maximum level vibration records could be identified. The tape loop was transferred to an auxiliary playback. A more detailed spectral analysis was accomplished using a Spectral Dynamics SDS-101A analyzer. The bandwidths of the two crystal filters were 5 and 20 cps and were selected for both fine resolution and for their even, rational ratios. The latter property was chosen to expedite bandwidth comparisons of rms outputs during evaluation of the broad band characteristics of the vibration samples.

The filtered output of the analyzer was fed into a Ballantine 320 true rms voltmeter. The voltmeter was placed in parallel with an oscilloscope. Output readings of each filter were taken from the Ballantine meter; peak readings were taken from the calibrated oscilloscope. The time constant of the meter was approximately one second, as was the effective tape sample length. The frequency spectrum was slowly scanned. At intervals, filter bandwidths were switched and rms outputs and the incremental changes were noted. If the spectrum were predominantly broadband and essentially flat over the filter bandwidths, one would expect that when switching from 5 cps to 20 cps, the rms meter output would increase by a factor of approximately two. This is because the rms output is proportional to the square root of the filter bandwidth.

A criterion for predominance was set at 1.6. That is, whenever the metered output showed an rms increase of 1.6 or greater (when switching from

5 cps to 20 cps) the sample was classed as being predominantly broad band. Instantaneous peak values were also noted during this procedure. In this way, samples of the spectrum were characterized as being either predominantly broad band or, alternatively, falling within the discrete frequency class.

The results of the bandwidth test were interesting. Above approximately 75 cps, filter switching produced, on the average, a two to one change in the rms readouts. Generally, the higher the frequency the stronger this broad band tendency. Conversely, as one approached approximately 20 cps (the basic firing rate of the guns), the bandwidth change showed little change in rms g level; note, however, that peak to rms ratios were about 4 to 1 in this frequency range. Also, peak to rms ratios were approximately 4 to 1 in the region of the antenna failure mode. Above this frequency, values occasionally ranged as high as 10 to 1.

Previous sinusoidal studies had isolated the antenna failure mode. This mode, occurring at approximately 490 cps, was well above the basic firing frequency. Thus further evaluation of the low frequency end of the spectrum was terminated. The remainder of the spectral studies were concerned with the vibration histories above approximately 100 cps.

C. STATISTICAL ANALYSIS

The bandwidth test is an indication of the broad band characteristics of the vibration field. It does not, however, give us details concerning the distribution of the amplitudes. The tape loop was fed, therefore, into a Gulton Ortholog probability density analyzer. The distribution was determined for each pickup, first as a velocity distribution and then through differentiation, as an acceleration distribution.

The analysis properties were as follows: Averaging time = 1 second, Analysis window = $.1 \sigma$, Window sweep rate = $.02 \sigma/\text{sec}$, Tape length = 1 second.

Figure 3 shows a plot of the probability density distribution for velocity and acceleration. For comparison, a normal or Gaussian distribution is superimposed over the figures. Only the vertical pickup record is shown. The remaining two vibration directions gave similar results.

Compared to the Gaussian (normal) form, the velocity and acceleration forms are slightly skewed to the left and right respectively but both curves resemble the normal distribution.

Differentiation of noisy vibration signals tends to emphasize the peaks of a velocity distribution. An examination of the acceleration curve shows this emphasis. The distribution of the peaks should have been greater than this - the inhibition of peak distributions resulted from the selection of a lower filter cutoff frequency (200 cps). This step was required in order to reduce the probability density loading tendency (occurring about the mean) because low level noise signals due to tape and instrumentation contributions were encountered. For the velocity distribution, the filter cutoff was switched to 2000 cps. Despite the bandwidth disparity of one decade, it is interesting to note that the basic shape of the acceleration curve

remains close to that of the velocity shape. This observation suggests that the distribution remains essentially constant over a wide range of frequency bandwidths.

It would have been instructive to examine the narrow band probability density distribution and the narrow band instantaneous peak to rms distribution. Time, however, did not permit such an analysis.

C. SAMPLING ERRORS

Since power spectral density measurements are the result of a statistical sampling process, as are the probability measurements, we now consider the sampling errors involved during both measurements.

Power Spectral Density

For true rms measurements and assuming bandwidth limited gaussian noise with zero mean, the normalized standard error for the mean square value estimate is:

$$e = 1/2\sqrt{BT}$$

where B is the analyzer effective noise bandwidth and T is the averaging time. Thus:

$$e = 1/2\sqrt{20} = 0.112$$

where B = 20 cps and T = 1 second.

From [1] we note that if $e \leq 0.2$, we are permitted to use the chi square distribution to indicate the confidence and the limits of the estimate. Noting that $n = 4BK$, where

n = degrees of freedom,
B = analyzer bandwidth,
K = T/2,
T = tape sample length,

and setting B = 20 cps and K = 1/2 sec, we have

$$n = 4(20)/2 = 40$$

Referring to confidence interval tables, one notes that one may be 90% confident that the measured mean square acceleration falls within 29% below or 51% above the true mean square value or, approximately, ± 2 db.

The statistical error, though not as small as desired, is suitable for the initial vibration estimate required. Note that the lowest error occurs when the largest bandwidth (20 cps) is used. The power spectral density values were largely determined from this bandwidth.

Probability Density

The error of the estimate is more difficult to state when using probability density analyzers. Nonetheless, by following current statistical procedures and examining the recorded distributions, we gain some insight into the measurement uncertainties of the analysis process.

The analyzer is an RC averager and the window (W) sweeps continuously in the normal mode of operation.

To inhibit statistical sampling errors, the sweep rate (S.R.) must be limited to the following criteria [2]:

$$S.R. \leq W/4K$$

The analyzer window width (W) is equal to .1σ and K is one second so that:

$$S.R. \leq .025 \sigma/\text{sec}$$

In actual practice the analyzer S.R. was set to .02 σ/sec, meeting the above requirement. We now consider the normalized standard error. From [2]:

$$e = 0.26 / \sqrt{W \hat{p}(x) \bar{V}_O T}$$

where: 0.26 = Empirical constant, T = Sample length, W = Analyzer window width, $\bar{V}_O = 2(f_c) = 2(200) = 400$ cps, and $\hat{p}(x)$ = probability density of the sample. Setting $\bar{V}_O = 400$, T = 1 sec, W = .1 σ; and selecting from the velocity record $\hat{p}(x)$, at one σ, equal to .12, we have:

$$e = 0.26 / \sqrt{(.1)(.12)(4)(100)(1)} = 0.118$$

With these chosen values, the normalized standard error is acceptably low - at least up to 1 σ. For example, over this range of vibration amplitudes, $e \leq 0.2$ and from ref [1] we conclude that we may assume a 95% confidence that the measured probability density is within ±2e of the true mean value. At one σ, this is ±24 percent.

What of the error for the acceleration probability density distribution? As previously mentioned, pre-filtering was required, resulting in a reduction of the sample bandwidth. Returning to [2] we select a modified form of the error equation which reflects this bandwidth restriction.

$$e = 0.17 / \sqrt{W \hat{p}(x) B T}$$

where: 0.17 = Empirical constant, B = Bandwidth = 200 cps, T = same as before, $\hat{p}(x)$ = prob. density of accel. sample. Repeating the former steps, we set B = 200 cps, W = .1σ, T = 1 sec, and $\hat{p}(x)$, at one σ, of .15 and obtain

$$e = 0.17 / \sqrt{(0.1)(.15)(10^{-2})2(10^2)(1)} = 0.17/1.73 = .098$$

Noting that $e \leq 0.2$ and referring to [1], we conclude that there is a 95% confidence that the measured value is within approximately 20% of true sample mean. The error, at one σ, is rather high but acceptable. However,

at approximately 3σ the error becomes very large. In fact, our criteria, $e \leq 0.2$, is no longer met at large amplitudes.

It should be noted that the error equation is approximate and does not adequately describe errors for extreme values - this is discussed in [2]. The error condition at large σ is probably less than the calculated values, and if this were of concern, one could have obtained the probability density (at extreme values) from the oscillographic records and then compared the distribution to the analyzer results. This was not done, however, and the acceleration probability density curve of Figure 3 was tentatively assumed to be sufficiently valid for estimation requirements.

To summarize, the bandwidth analysis indicated a broad band vibrational field and the probability density analysis suggested that random noise vibration would be more desirable for gunfire simulation than the other alternative, namely sinusoidal vibration.

The data from each of the three channels were converted to mean square values and divided by the bandwidth. The power spectral density in g^2/cps was plotted against frequency. The plotted points were enveloped, leading to a vibration spectrum geometrically similar but not equal to the spectrum shown in Figure 4 - the power spectrum magnitudes were modified as is explained later.

E. STRUCTURAL CHARACTERISTICS

The pickups were mounted on the main structure, at the gun recoil site. The mounting structure of the antenna appeared similar. Further, impact tests indicated no appreciable resonances (audible) below approximately 75 cps. It was, therefore, conditionally assumed that the average structural admittance of both sites was similar.

F. TEST CURVE CORRECTION

The vibration field recorded by the pickups represents a very severe level - but perhaps not the region of the severest levels. Since the antenna is located approximately one foot fore of the cannon muzzles, we would expect blast contributions to be significant, possibly resulting in a combinational vibration field equal to or greater than at the pickup site. Because of this unknown, and again assuming structural similitude, we add approximately 2db to the envelope of the gunfire spectrum previously derived.

This, then, resulted in the gunfire simulation spectrum shown in Figure 4.

G. TIME TO FAILURE

A number of samples were subjected to the vibration spectrum. For vibration and spectral shaping, a Ling A-300B shaker was used with a 24 channel equalizer. The acceleration peaks were clipped at approximately 3 to 4 times the rms. Detailed discussions concerning the isolation of the failure mode and the determination of the non-linear nature of the failure response

(it was highly non-linear) are beyond the scope of this report. However, it is important that the laboratory time-to-failure correlate with service failure as a necessary link in determining the propriety of assumptions used during data analysis and the accuracy of the test spectrum synthesized.

Times to failure (averaged over 4 antennae) were approximately four minutes. In comparison, actual gunfire time to failure, obtained from field reports, ranged from 1 to 4 minutes.

These test times to failure were considered to be sufficiently in agreement with field failure times to warrant the continued use of the test spectrum of Figure 4. This spectrum, therefore, was used without variation during the development of the dynamic damper.

III. THE VIBRATIONAL PROBLEM AND POSSIBLE SOLUTIONS

A. VIBRATIONAL CHARACTERISTICS OF THE UNDAMPED ANTENNA UNDER LOW INTENSITY SINUSOIDAL EXCITATION

The basic antenna geometry is illustrated in Figures 5 and 6. In order to determine the nature of the response characteristics of the antenna in some detail, the antenna was attached to an electro-dynamic shaker by means of a simple fixture and an accelerometer was attached to the inner surface as shown in Figure 5. It is seen from the typical response spectra shown in Figure 7 that the response is essentially unimodal, with a single resonant frequency occurring at about 490 cps, having an amplification factor of about 30. The vibrational mode is predominantly diaphragmatic with the electrical connector, the bulkhead connector and the center of the flush-mounted glass- fiber surface vibrating in phase at a frequency of about 490 cps. The region of highest cyclic surface stress is on the interior, at the edge of the dish-like inner surface and this is where the fatigue failures tended to occur, as shown in Figures 5 and 8. The cyclic stresses at most other points were small.

B. DAMPING TECHNIQUES AND THEIR APPLICABILITY

It has long been customary in the aerospace industry, when one is confronted with a severe vibrational problem, to follow the following general procedure: (i) stiffen the structure and/or (ii) add a surface damping treatment consisting of a layer of some readily available viscoelastic material. In many cases, of course, one or other of these ad hoc approaches deals adequately with the problem and the matter is forgotten. The particular problem presently under consideration, however, is very much akin to the classical acoustical fatigue problem insofar as the excitation covers so wide a band of frequencies that stiffening the structure cannot get one out of the range of significant excitation and, in addition, only the most careful use of damping is of any value.

Various attempts to stiffen the antenna were made by the manufacturer. One attempt at a solution to the problem involved filling the antenna with a polystyrene type foam, the effect of which was to raise the resonant frequency to about 670 cps and increase the amplification factor to about 40. In tests under the simulated operational environment performed at the Flight Dynamics Laboratory, no improvement in fatigue life was noted. Another attempt to stiffen the structure involved the joining of the arm of the electrical connector to the outer rim by means of a welded clamp. The fatigue life was not improved. A glance at the excitation spectrum under the simulated environment in Figure 4 shows that one would have to raise the resonant frequency to at least 1000 cps in order to lie outside the range of significant excitation, so that the stiffening techniques adopted were never likely to succeed.

Surface damping treatments depend for their effectiveness on the existence of large areas of high cyclic strain on the surface. In this instance, since the mode of vibration was predominantly diaphragmatic, no large strains existed anywhere apart from the small region near the rim where failure occurred. For this reason, no surface damping technique was usable.

The only significant response, in fact, was at the electrical connector and bulkhead. Therefore, the only damping techniques likely to be of use were those utilizing this amplitude of vibration. The only such techniques known are the viscoelastic link [3,4] and the tuned damper [3,5,6]. The viscoelastic link technique could not be used since there appeared to be no place to which the link could be readily connected. On the other hand, adequate space existed around the electrical connector for a small tuned damper to be located. The development of a tuned viscoelastic damper, attached around the electrical connector, was therefore made the aim of the investigation.

IV. INITIAL DAMPER DESIGNS AND THEIR TESTING

The initial damper designs were built on a largely ad hoc basis, utilizing viscoelastic materials readily available within MAMD regardless of whether they were the best possible materials for the job or not. The purpose of this policy was to gain insight into the actual material properties needed to achieve high damping over a wide temperature range and the ability to withstand the simulated and operational environments in all respects.

A. PROTOTYPE 1

The first material to be seriously considered was a polyvinyl chloride copolymer known as VPCO-15080, manufactured by Farbwerke Hoechst AG, Frankfurt, Germany. Some samples of the material were available in MAMD in sheets about 0.1 inch thick and the damping properties, described in reference [7] and drawn out in Figure 9, appeared to be suitable for operation at temperatures up to 150°F, which was the initial target temperature. A damper of the geometry shown in Figure 10 was designed and built by MAMD. This geometry formed the basis for all subsequent damper designs. Two layers of VPCO-15080 were joined by means of Eastman 910 (A modified cyanoacrylate monomer modified with a thickening agent and plasticizer, supplied by Armstrong Cork Co. and Eastman Chemical Products, Inc.) cement and the material, cut to shape as shown, was attached to the inner brass clamp by means of the same adhesive. A brass tuning mass was then attached to the outer surfaces of the viscoelastic material. Various tuning masses were used and, for each, the damper was attached to the electrical connector by means of the inner clamp and the connector was then attached to the antenna as in Figure 11.

Using the miniature accelerometer attached to the inner surface of the antenna, frequency response curves were obtained for various harmonic input acceleration levels, temperatures and tuning masses. Typical response spectra for the antenna with and without a damper are shown in Figure 12. A typical graph of amplification factor A , defined as the ratio of the greatest resonant response acceleration to the input acceleration, against temperature for a tuning mass of 50 grams is shown in Figure 13. It was found that a 50 gram tuning mass gave the best overall reduction of response in the temperature range 50°F to 150°F, and the damper with this particular mass was selected for further testing under the simulated operational environment.

Under continuous random excitation the VPCO damper performed well for about 15 minutes without failure, and the test was stopped at this point. This was due to the fact that the damper heated up excessively and the material became too soft. It was recognized only later that a more accurate simulation of the operational environment would be bursts of not more than 30 seconds of random excitation with rest periods between bursts. This more realistic testing procedure reduced temperature rises in the material. The fact that the VPCO damper even held together for 15 minutes under this severe overtesting implied, therefore, that it would probably have worked well under the more realistic burst excitation conditions.

Even so, however, the damper was not entirely satisfactory since (i) supplies of the material were limited and a great deal of time might have been lost trying to obtain more from Germany, (ii) the proper adhesives to give a completely trustworthy bond at temperatures up to 150°F were not known and (iii) the resonant amplification factor increased rapidly at temperatures below 50°F and above 150°F, a possibly serious matter in the event of aircraft utilization outside this range. While, therefore, this initial damper design was a partial success further efforts were made to find more satisfactory viscoelastic materials.

It became clear from tests on these prototype dampers that the variables involved, namely (i) tuning mass, (ii) viscoelastic element dimensions and (iii) material properties were too great in number for a simple design procedure to be adopted. A great simplification could be achieved, however, if the material damping properties were simple functions of temperature, preferably varying very little. For this purpose, the ideal material would have a high loss factor, not less than 0.2, and a Young's modulus, or shear modulus, which did not vary rapidly with temperature in the range of interest. It is evident that the VPCO-15080 material did not satisfy this requirement. In general, the operating temperature range should lie within the so-called "rubbery" phase of the viscoelastic material which lies above the glass-transition temperature. The search for materials for which the rubbery region lies within the temperature range of 50°F to 200°F will be discussed in the next chapter.

V. PROTOTYPE AND PRODUCTION DAMPER DESIGNS USING NITRILE RUBBERS

A. PROTOTYPE 2

In view of the considerations discussed in the previous chapter, a damping material was sought which had a Young's modulus as nearly independent of temperature as possible in the range 50°F to 200°F and as high a loss factor as possible. The most promising material initially found was the very high acrylonitrile containing rubber known as Paracril-D, manufactured by the U.S. Rubber Company. The formulation used is given in Table 1. This material is resistant to oils, gasoline and many acids so that this environmental problem, at least, did not have to be taken into account. The damping properties of Paracril-D, measured by MAMD just prior to the materials search [8,9], are illustrated in Figure 14. It is seen that the Young's modulus changes by a factor of about 2 only, between 80°F and 200°F, compared with a factor of about 10 for VPCO-15080 over the same temperature range.

Using sheets of Paracril-D cured with dicumyl peroxide, supplied by MANE, a damper of the geometry shown in Figure 15 was hand built by MAMD using Eastman 910 cement as an adhesive. On the basis of the experience acquired previously, a tuning mass of 45 grams was chosen and was found to give acceptable damping performance. Response measurements were made in the usual manner and graphs of amplification factor against temperature are plotted in Figure 16(a). It is seen that amplification factors of less than 10 were obtained over a 100°F temperature range, compared with only about 70°F for the VPCO-15080 damper. It was thought that the performance could be improved further by reducing the tuning mass to 35 grams, a fact which was confirmed when a mold specimen was manufactured as described for Prototype 3. The design was frozen at this point, and an effort was made to refine the fabrication procedure to ensure damper uniformity and reproducibility.

A single cavity mold was designed to allow for precision molding and bonding of four separate blocks of viscoelastic material between the inner brass clamp and the outer brass tuning masses. The mold, illustrated in Figure 17, consists of a base plate with spacers, a centrally located removable post to position and locate the clamp, a retaining plate which positions the outer tuning masses and a top mold plate.

The assembly of the base plate, the retaining plate and the post is shown in Figure 17. The four elastomer mold cavities are provided automatically as the brass pieces are placed in position. Fabrication of the damper was accomplished by placing the uncured elastomer in the cavities and molding in a hydraulic press at a predetermined pressure and temperature. The stainless steel mold and brass components were pre-treated to ensure proper bonding of the elastomer and brass components. The finished damper, as it is removed from the mold, is also shown in Figures 18 and 19.

Minor modifications were later made to both mold and tuning masses in order to compensate for stiffer viscoelastic materials, relieve stress concentrations at the elastomer - brass bond and to increase the bonding area. These changes will be discussed in the appropriate sections.

B. PROTOTYPE 3

On the basis of the frozen design, illustrated in Figure 19, a mold was prepared as already discussed and all future dampers were made by curing the viscoelastic material, under high temperature and pressure, in the mold so as to obtain a far better bond to the metal surface than could be achieved with normal adhesives. The metal from which the inner clamp and the tuning mass had been machined, in most of the hand-made dampers, was brass. Hitherto, this choice had been made only because of the convenience and ease of working associated with this metal but the choice was now particularly appropriate since many nitrile rubber formulations can be simultaneously cured and bonded to brass without auxiliary adhesives. The first Paracril-D mold specimen was cured using a sulfur curing system without an adhesive. It was found, however, that the bond was inadequate and, on the next attempt, the brass surfaces were (i) sand blasted using medium particle size flint shot, (ii) the embedded particles were removed by means of a stream of tap water and an oil-removing solvent such as acetone or methylethyl ketone and (iii) wiped dry with a clean piece of cheese cloth. A commercial adhesive (Chemlok 220, manufactured by the Hughson Chemical Company) was then applied to the surfaces to be bonded. Care was taken to avoid touching the cleaned surfaces with the hand. If the surfaces were particularly rough, two applications were made.

When the adhesive had touch dried, the brass components of the damper were placed in position in the cold mold, the uncured Paracril-D was pressed into the appropriate spaces and the entire mold unit was put into a press at a temperature of 310°F and a pressure of 100 psi for 30 minutes. The cured dampers were then removed from the hot mold and dropped into water to cool them rapidly and prevent further high temperature curing.

For ready identification, the mold specimens were designated TD-1, TD-2 and so on. Of the first two mold specimens, TD-1 and TD-2, TD-1 was defective and TD-2 was tested under sinusoidal excitation in the usual manner. The graph of amplification factor against temperature for a 10-g input level only is shown in Figure 16(b). When a strip of brass weighing 5 grams was added to each tuning mass by means of Eastman 910 cement the amplification factor values were found to lie along the same curve as that of prototype 2, as seen in Figure 16(a), indicating that the mold specimens were indeed accurate copies of Prototype 2 apart from the new tuning mass of 35 grams.

It will be noted that, for TD-2, the amplification factor was less than 10 between 80°F and 200°F at the 10-g input level, a 120°F temperature range. For this reason, there is little doubt that a damper utilizing Paracril-D could have been built to operate effectively under the operational environment but another related material, namely Paracril-BJ, performed so much better that the effort was now concentrated on that material.

C. PROTOTYPE 4

The measured data for TD-2, shown in Figure 16(b), indicates that the amplification factor is less than 10 between 80°F and 200°F and such performance appeared to be acceptable. However, it was thought that a small extra margin of safety in the form of reduced amplification factors below 80°F would be useful. For this purpose, a medium acrylonitrile rubber, known as Paracril-BJ, was considered. At the time no data concerning the damping properties of Paracril-BJ was available, but it was thought that, as the glass transition temperature was somewhat lower than that of Paracril-D, the general effect would be a shift of the amplification factor versus temperature curve to the left. The next seven specimens, TD-3 to 9, were therefore made using Paracril-BJ, in exactly the same way as for Paracril-D and shaker tested in the usual manner. Typical values of the amplification factor at various temperatures are plotted in Figures 20, 21 for TD-3 and 4. It is seen that the performance change is significant and the temperature range for which the amplification factor falls below 10 is now from 30°F to 200°F. The increased temperature range of measurements for TD-4 was obtained by placing an environmental chamber over the specimen in the shaker.

An explanation for the remarkable improvement in the damping performance of the dampers with Paracril-BJ would not be amiss and, for this reason, the damping properties of Paracril-BJ were subsequently evaluated by MAMD and provisional results are plotted in Figure 22. It is seen that, while the data is somewhat similar to that for Paracril-D, significant differences occur, namely (i) between about 50°F and 200°F the rate of change of Young's modulus with temperature is much lower than for Paracril-D, (ii) the rate of change of Young's modulus with temperature near the glass transition temperature is far greater than for Paracril-D and (iii) the peak loss factor is far higher than for Paracril-D and varies far more rapidly with temperature in the vicinity of the glass transition temperature.

One of the dampers was now taken to the random shaker facility and tested under the simulated operational environment. The specimen failed rapidly in shear across the center of a viscoelastic element. Failure was due to inadequate strength of the material and it was necessary to take steps to increase this strength. This could be accomplished by adding Carbon or Polystyrene to the Paracril-BJ blend prior to curing. Of the dampers TD-3 to TD-9 made previously, one was kept for future testing, another was remade using Paracril-BJ containing 50 PHR (parts per hundred parts rubber) super abrasive furnace carbon black (SAF black), another (TD-7) was remade using Paracril-BJ with 10 PHR Polystyrene and the remainder were set aside. The damper containing Paracril-BJ with 50 PHR Carbon was tested first.

D. PROTOTYPE 5

The damper containing Paracril-BJ with 50 parts PHR Carbon, to the formulation given in Table 2, was of the same geometry as Prototype 3. The sinusoidal vibration tests indicated that the amplification factors at resonance were far higher than those for Prototype 4 and little testing was carried out for this reason. The available data is plotted in Figure 23, taken in subsequent measurements. The damper failed under the simulated random

environment, due probably to the high amplification factors. Subsequent evaluation of the damping properties of Paracril-BJ with 50 parts PHR Carbon, illustrated in Figure 24, show that the reason for this poor performance is the fact that the carbon increased the Young's modulus of the material (and also, presumably, the shear modulus) over the operating temperature range. Re-tuning could have been achieved by increasing the tuning mass but this would have involved re-making the mold, a solution which was not willingly accepted. Strength measurements indicated that, at room temperature, the tensile strength of Paracril-BJ was about 600 psi, that of Paracril-BJ with 25 parts PHR Carbon was roughly doubled and that of Paracril-BJ with 50 parts PHR Carbon was roughly tripled. It was therefore decided instead to evaluate the performance of a damper using only 25 parts PHR carbon in the Paracril-BJ since it was thought that this particular material blend had sufficient strength and would not affect the amplification factors so severely. This particular damper, which turned out after modification to be the most successful, will be discussed presently.

E. PROTOTYPE 6

Prior to the making of the damper utilizing Paracril-BJ with 25 parts PHR Carbon, the damper TD-7 utilizing Paracril-BJ with 10 parts PHR Polystyrene was tested. Again, the geometry was the same as that for Prototype 3. The measured amplification factors for various temperatures and input accelerations are plotted in Figure 25. It is seen that the effect of the Polystyrene was to reduce the amplification factors between 50°F and 200°F, with less change below 50°F. This is due to the fact that the Polystyrene has a high glass transition temperature and would tend to increase the loss factor of the material slightly at high temperatures. The damper TD-7 was then tested under the simulated operational environment and failed in a few seconds indicating that the Polystyrene had not significantly increased the material strength. This particular material was not investigated further for this reason.

F. PROTOTYPE 7

The re-made dampers TD-5 and TD-8, utilizing Paracril-BJ with 25 parts PHR Carbon, were now evaluated under sinusoidal excitation at 10 and 20 g input levels in the usual manner. TD-6 was remade but was not tested since the results for TD-5 and TD-8 were sufficiently consistent, as is seen in Figure 26. It is seen that, for Prototype 7, the amplification factors were less than 10 between 100°F and 250°F at the 10-g input level. The degradation in performance, relative to Prototype 4 using Paracril-BJ, is due to the effect of the carbon on the stiffness of the material. The increased stiffness properties of the material, evaluated subsequently by MAMD, are shown in Figure 27. The general increase of stiffness relative to that of Paracril-BJ will be noted. The damper could be re-tuned by increasing the tuning mass, as was considered for the dampers using Paracril-BJ with 50 parts PHR Carbon, but this was not possible without altering the mold, which would be both time consuming and expensive. An alternative procedure for re-tuning was adopted to produce Prototype 8 and this will be discussed presently.

However, the damping performance of Prototype 7, while not as good as that of Prototype 4, was still considered to be reasonable and the dampers TD-5 and TD-6 were consequently tested on the Random Shaker Facility to determine whether the strength problem had been solved, or not, before any further design changes were made.

For TD-5, under continuous random excitation, the damper lasted for 105 seconds and the damper material temperature had risen from 100°F to 175°F when the test was stopped. This high temperature was the cause of failure, since the strength of the material decreased with rising temperature. In view of this, TD-6 was subjected to the excitation in short bursts in order to simulate more accurately the actual operational conditions. The first burst was 13 seconds long and was followed by nine bursts each 30 seconds long, during which the temperature rose to about 130°F and sufficient rest was allowed between bursts for the temperature to fall to 100°F. This was followed by bursts of 60 seconds each, during which the temperature rose to the higher figure of about 150°F. Again, rest periods were allowed for the temperature to fall to 100°F between bursts. After a total testing time of 5 minutes and 43 seconds, a crack was noticed close to the rubber to brass bond at a corner of one of the viscoelastic elements. This crack traveled very slowly under the sixty second burst conditions and had traveled about half way across the material element when the test was stopped after 8 minutes and 43 seconds. This lifetime was not exceptionally great, but it did demonstrate the great increase in strength of the rubber and enabled a number of necessary design changes to be identified. These were, (i) the use of rectangular rubber elements caused stress concentrations at the corners, which could be eliminated by curving the free edges, (ii) the vibration levels could be reduced somewhat if the amplification factor were reduced by re-tuning the damper properly and (iii) shear strains should be reduced as much as possible. Items (ii) and (iii) could be accomplished by increasing the material thickness, as is discussed for Prototype 8.

G. PROTOTYPE 8

In view of the information derived from Prototype 7, the mold was slightly modified to give a finite radius along the free edges of the viscoelastic material elements, and in order to reduce the stiffness of the viscoelastic elements and reduce the shear strain, slots were machined out of the tuning masses to accommodate deeper material elements. The new geometry is illustrated in Figures 28 to 31, and this was the geometry finally adopted for all subsequent dampers. Again, the material used was Paracril-BJ with 25 parts carbon. The dampers TD-6, TD-8 and TD-9 were re-machined to this new geometry and tested under sinusoidal excitation as usual. Graphs of amplification factor against temperature of input levels of 10-g and 20-g are shown in Figure 32. It is seen that the effect of reducing the stiffness of the viscoelastic elements is, as would be expected, much the same as for increasing the tuning mass. However, no change in the mold geometry was involved.

The dampers were then subjected to the simulated operational environment. TD-8 was subjected to 30 second bursts of random excitation with rest periods between each burst to allow the viscoelastic material temperature to return to 100°F. At the end of each burst, the material temperature had risen to

about 125°F. The damper failed after about 6 minutes due to a failure in the adhesive. TD-9 was then subjected to the same environment. For the first 10 minutes, the material was allowed to return to 100°F after each burst and rose to about 120°F during each burst. For the next 10 minutes, the temperature was allowed to fall only to 120°F between bursts and peak temperatures near the end of each burst reached about 135°F. For the last 10 minutes, the temperature was allowed to fall to about 130°F between bursts and peak temperatures reached over 140°F. The damper had not failed at the end of this time and the test was discontinued since it was clear that, excluding failure due to poor adhesion, no trouble would be encountered. Care was subsequently taken to ensure that adhesion was perfect for each damper and doubtful dampers were remolded.

It was now clear that, with careful bonding, the design was performing satisfactorily for long periods of time under the properly simulated operational environment. The dampers TD-10 onwards were therefore, to all intents and purposes, production dampers and no further design changes were made. An antioxidant was added to the rubber used in all production dampers to protect it from possible oxidation degradation.

The first batch of dampers comprised TD-10 through TD-17 inclusive, and these were tested under sinusoidal excitation. Dampers TD-11, 12, 13, 15 and 17 were sent for field testing in October 1966 and, on the basis of field test data returned in January 1967, more dampers were manufactured. Graphs of the amplification factor against temperature for several input acceleration levels are plotted in Figures 33 and 34 for the dampers measured.

VI. FIELD TESTS

On 12 October 1966, five tuned dampers were sent for field testing. Included in the package with the dampers was a letter of explanation, instruction sheets and data forms for the reporting of test results.

On 26 January 1967, field test data was returned to MAMD. Apparently, no problems with installation had been encountered, indicating that the design of the dampers was satisfactory in that respect.

Detailed analysis of the returned field test data form by MAMD revealed several interesting features. Principal among these were the durability of the dampers themselves and the high variability between the results for the different dampers.

The variation between the lives of the various damper antenna combinations was high, ranging from 41.6 hours to over 105.5 hours but, in general, it was possible to relate these figures to the performance of the individual dampers under sinusoidal excitation. For example, TD-11 had the highest amplification factor at resonance and also gave the shortest antenna life. Figure 35 shows a graph of the resonance amplification factor A against temperature at a 20-g input level and Figure 36 shows the antenna life in hours as functions of this amplification factor. It is seen that, although the number of points is small, a characteristic S-N curve is produced. The laboratory data marked corresponds to all measurements taken in the temperature range 80°F to 170°F, within which the performance of the dampers did not vary greatly with temperature. It was thought that the true operating temperature would lie within this range.

VII. CONCLUSIONS

The main conclusions arrived at as a result of the tuned damper development program, apart from the solution of the field problem itself, are:

- (i) It is possible to produce tuned damping devices which will effectively reduce vibration damage in a structure over a wide range of temperatures by utilizing the visco-elastic material in the so-called "rubbery region."
- (ii) That adequate strength can be introduced into the material and the bonds to withstand a very severe vibrational environment. This can be accomplished by modification of the visco-elastic material, suitable primers and adhesives and by giving attention to the geometry in detail.

REFERENCES

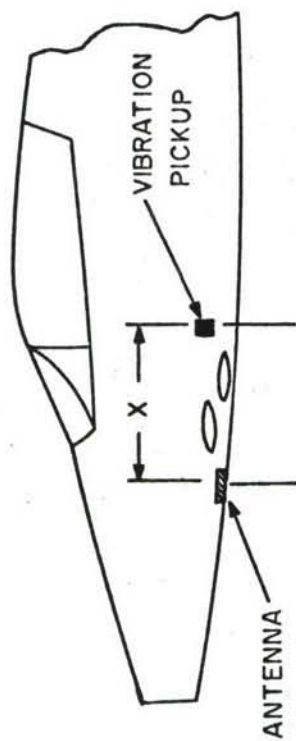
1. Bendat, Julius S. and Allen G. Piersol, Measurement and Analysis of Random Data, John Wiley & Sons, Inc., p. 242.
2. "Advanced Concepts of Stochastic Processes and Statistics for Flight Vehicle Vibration Estimation and Measurement," ASD-TDR-62-973, December 1962.
3. Jones, D.I.G., "Some Aspects of the Analysis of Damping and Vibration in Simple Structures," AFML-TR-65-151, December 1965, pp 82-90.
4. Jones, D.I.G. and A.D. Nashif, "Damping of Structures by Means of Visco-elastic Links," Shock and Vibration Bulletin 36, Part 4, April 1967, pp 9-24.
5. Henderson, J.P., "Energy Dissipation in a Vibration Damper Utilizing a Visco-elastic Suspension," Shock and Vibration Bulletin 35, Part 7, April 1966.
6. Jones, D.I.G., A.D. Nashif, and R. Adkins, "Effect of Tuned Dampers on Vibrations of Simple Structures," AIAA Journal, Vol. 5, No.2, February 1967.
7. Oberst, H. and Schommer, A., "Optimization of Visco-elastic Damping Materials for Specific Structural Composite Applications," in Acoustical Fatigue in Aerospace Structures, eds. W. J. Trapp and D. M. Forney, Jr., Syracuse University Press, 1965, pp 599-616, Figure 2.
8. Owens, F.S., "Elastomers for Damping Over Wide Temperature Ranges," Shock and Vibration Bulletin 36, Part 4, April 1967, pp 25-35.
9. Nashif, A.D., "New Method for Determining Damping Properties of Visco-elastic Materials," Shock and Vibration Bulletin 36, Part 4, April 1967, pp 37-47.

TABLE 1

Nitrile Rubber Formulations

Material	Prototype Damper Number						
	5	6	7	8	9	10	11
Paracril-D	100	100					
Paracril-BJ			100	100	100	100	100
Polystyrene					10		
Zinc Oxide	10	10	10	10	10	10	10
Dicumyl Peroxide	3						
Stearic Acid			1.5				
Sulfur		1.5	1.5	1.5	1.5	1.5	1.5
Benzothiozyl Disulphide		1.5	1.5	1.5	1.5	1.5	1.5
Antioxidant 2246*							1.0
SAF Black				50		25	25
Cure Temp. °F	280	310	310	310	310	310	310
Cure Time, mins	60	30	30	30	30	30	30

*American Cyanamid Co. trademark for 2,2'-methylenebis (4-methyl-6-tertiary-butyl phenol).



$X = 42''$ (ESTIMATED)

Figure 1. Longitudinal Spatial Relationships of Vibration Pickup Antenna

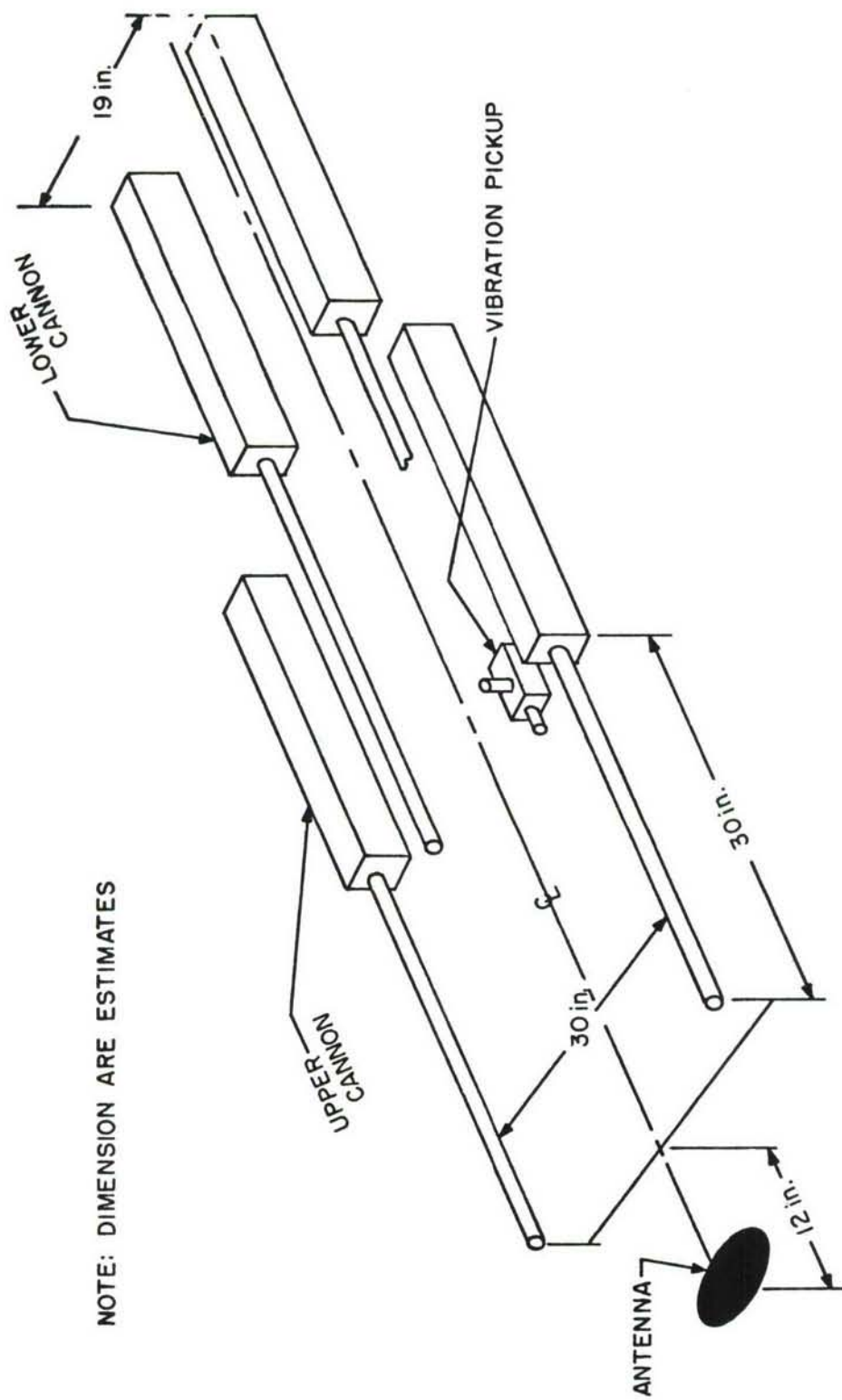


Figure 2. Relative Locations of Cannon, Pickups and Antenna

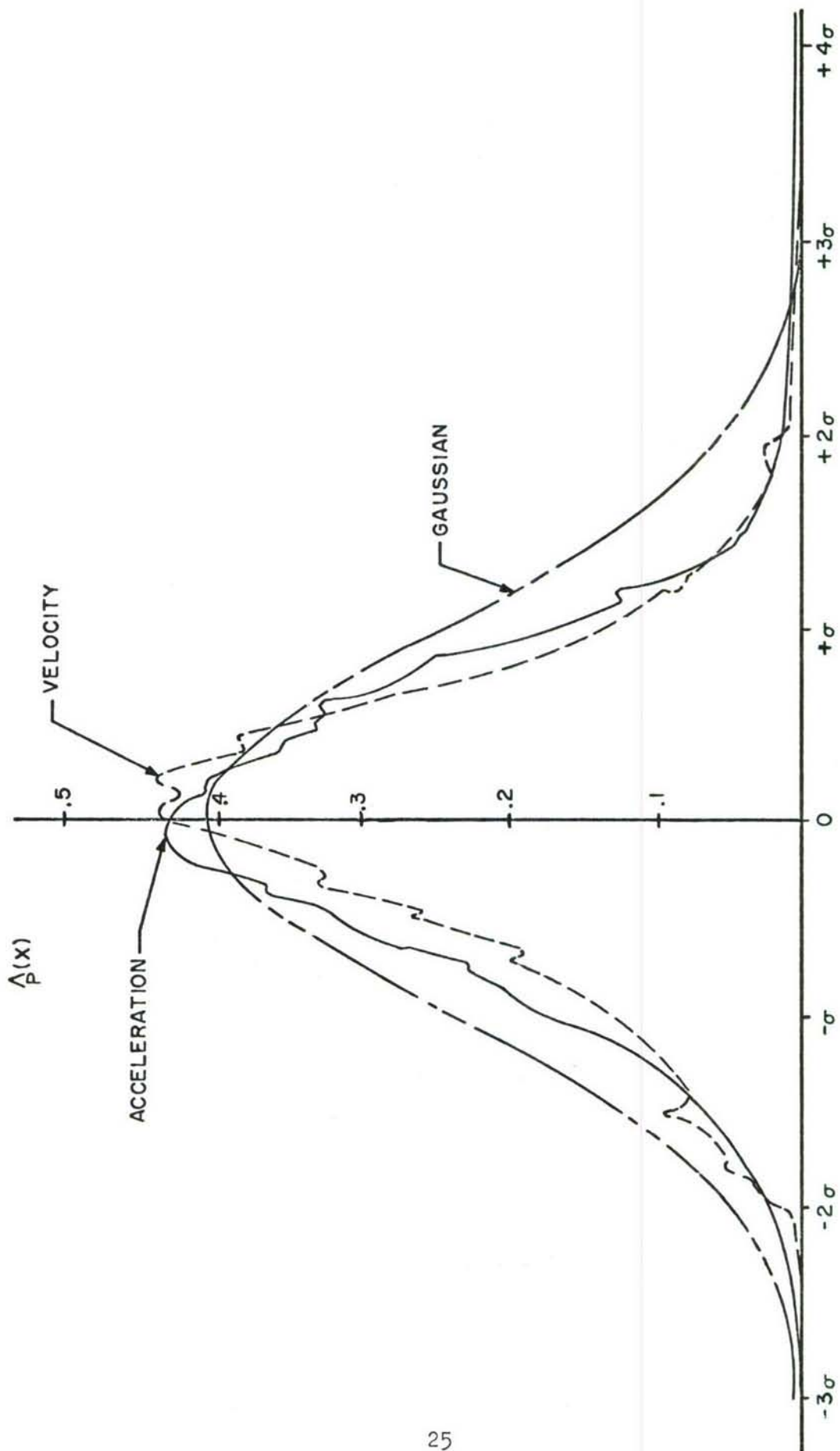


Figure 3. Probability Density Distribution of F-100 Gunfire Record

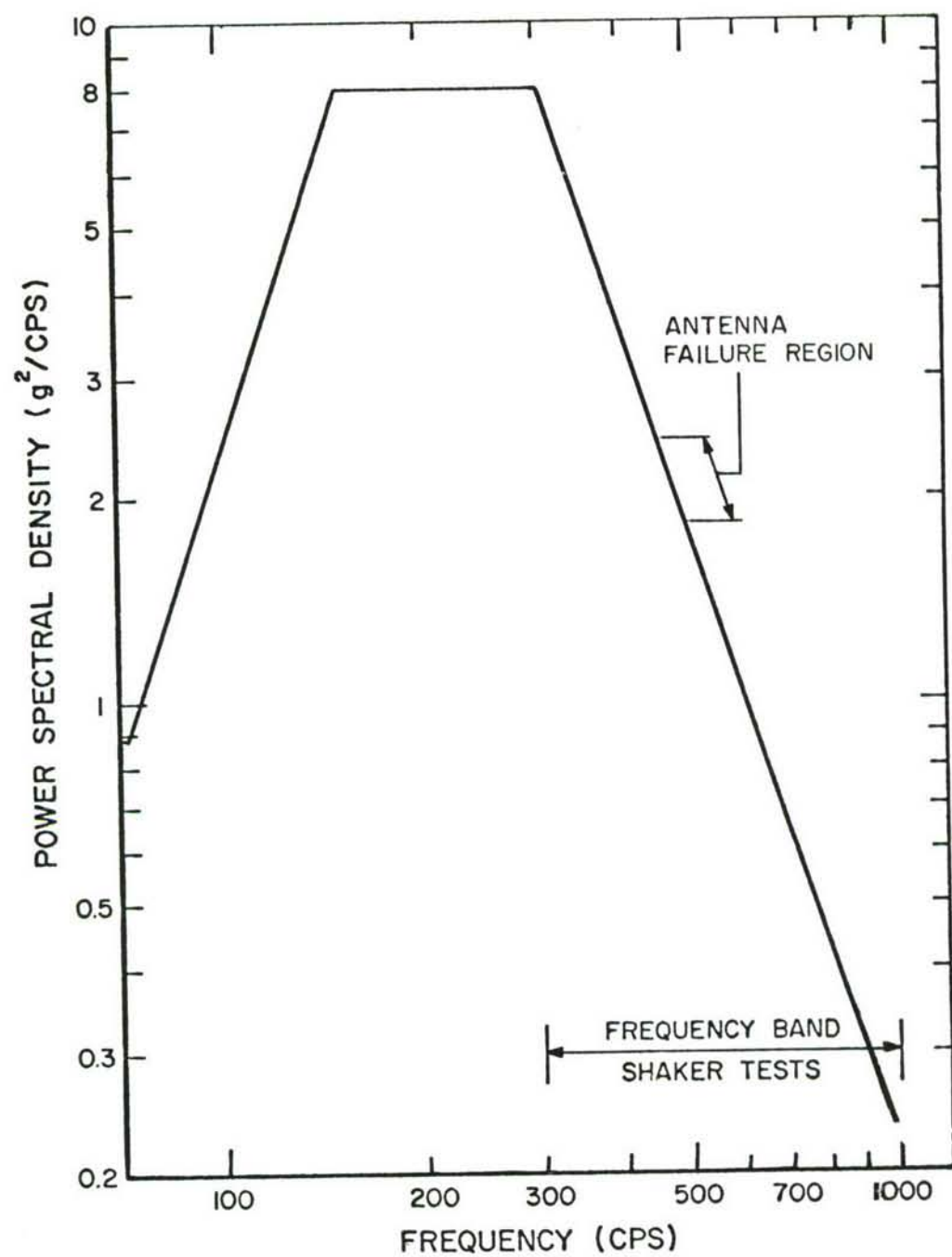


Figure 4. Derived Broad-Band Random Spectrum

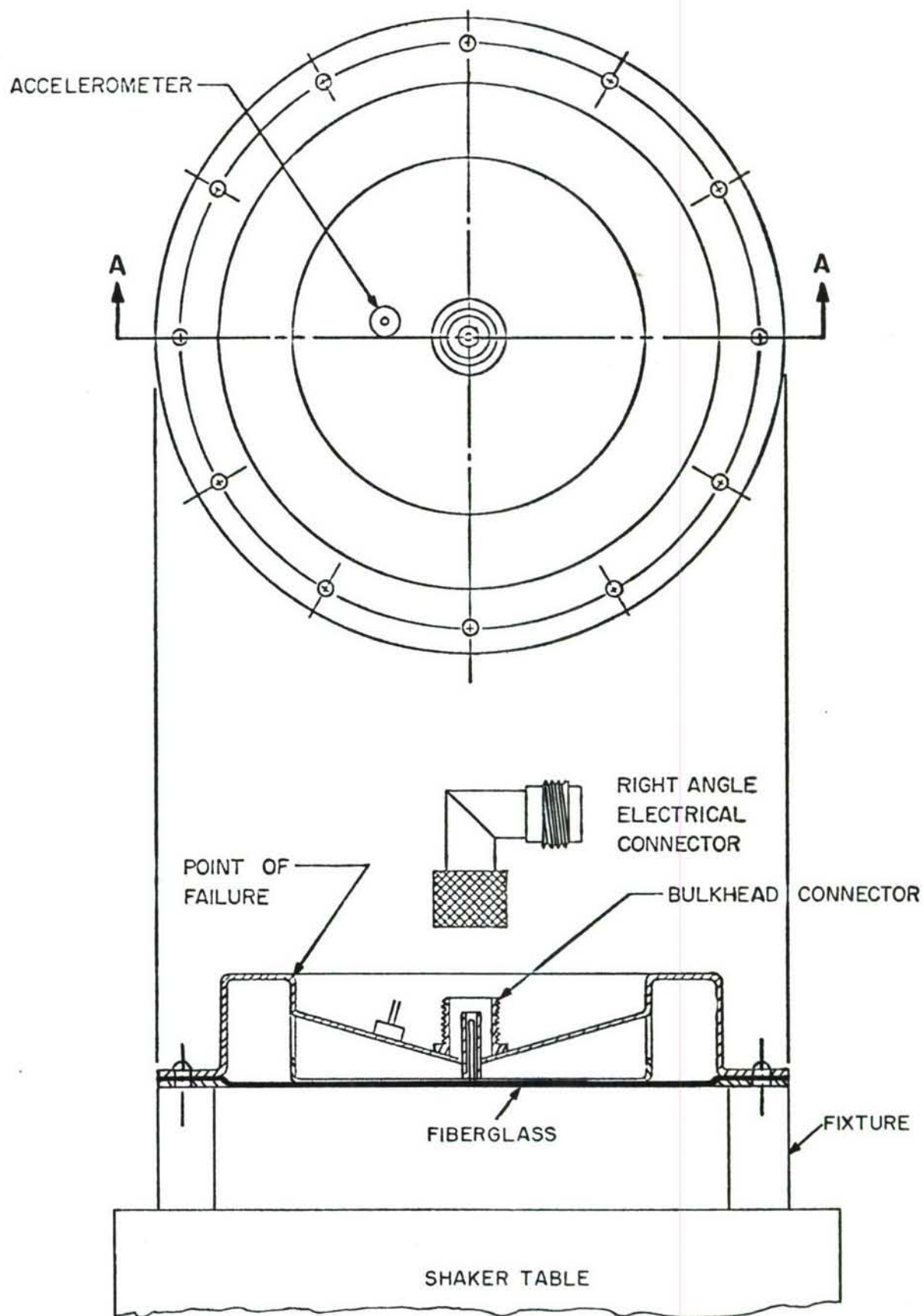


Figure 5. Schematic of Radar Antenna

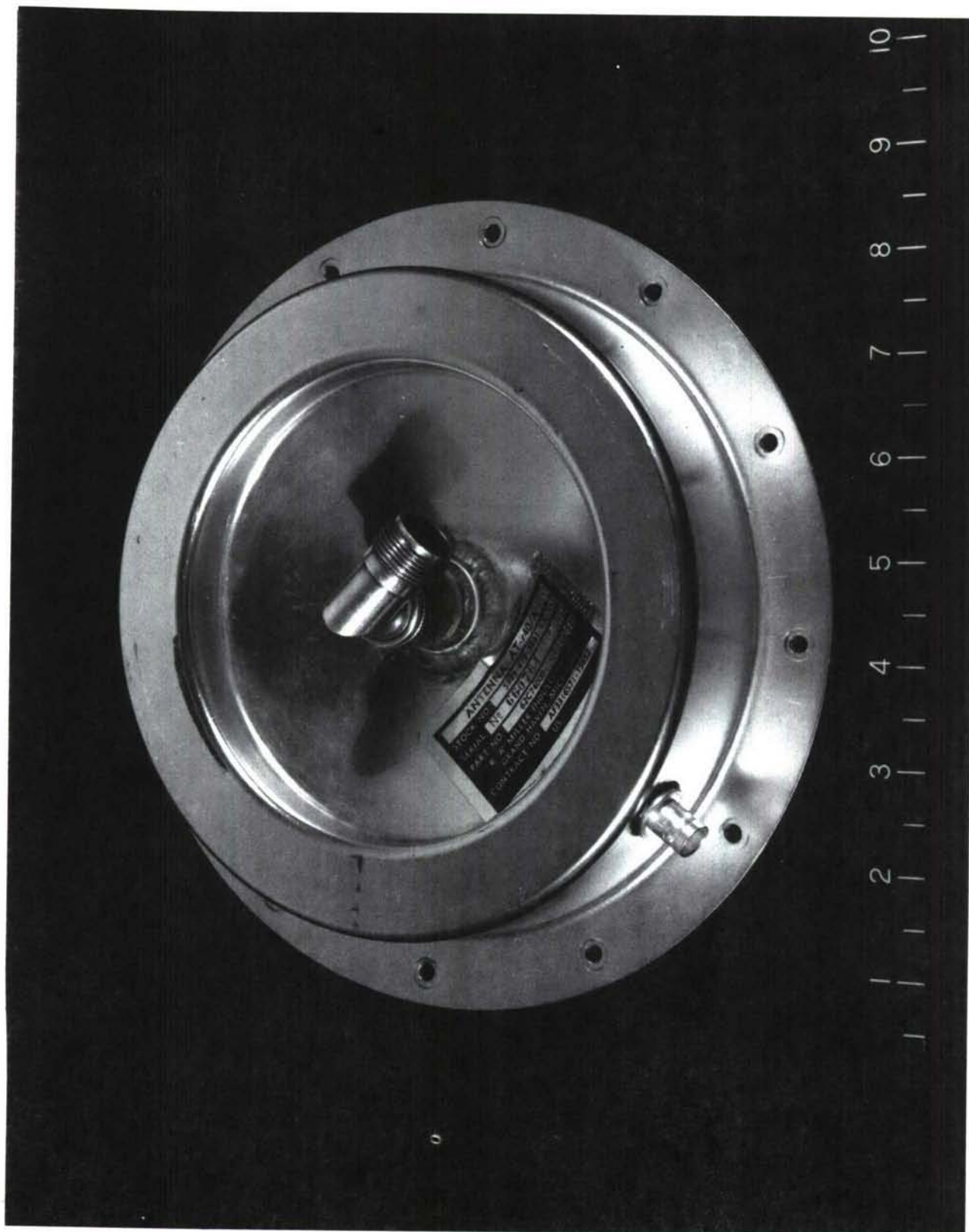


Figure 6. Photograph of Antenna

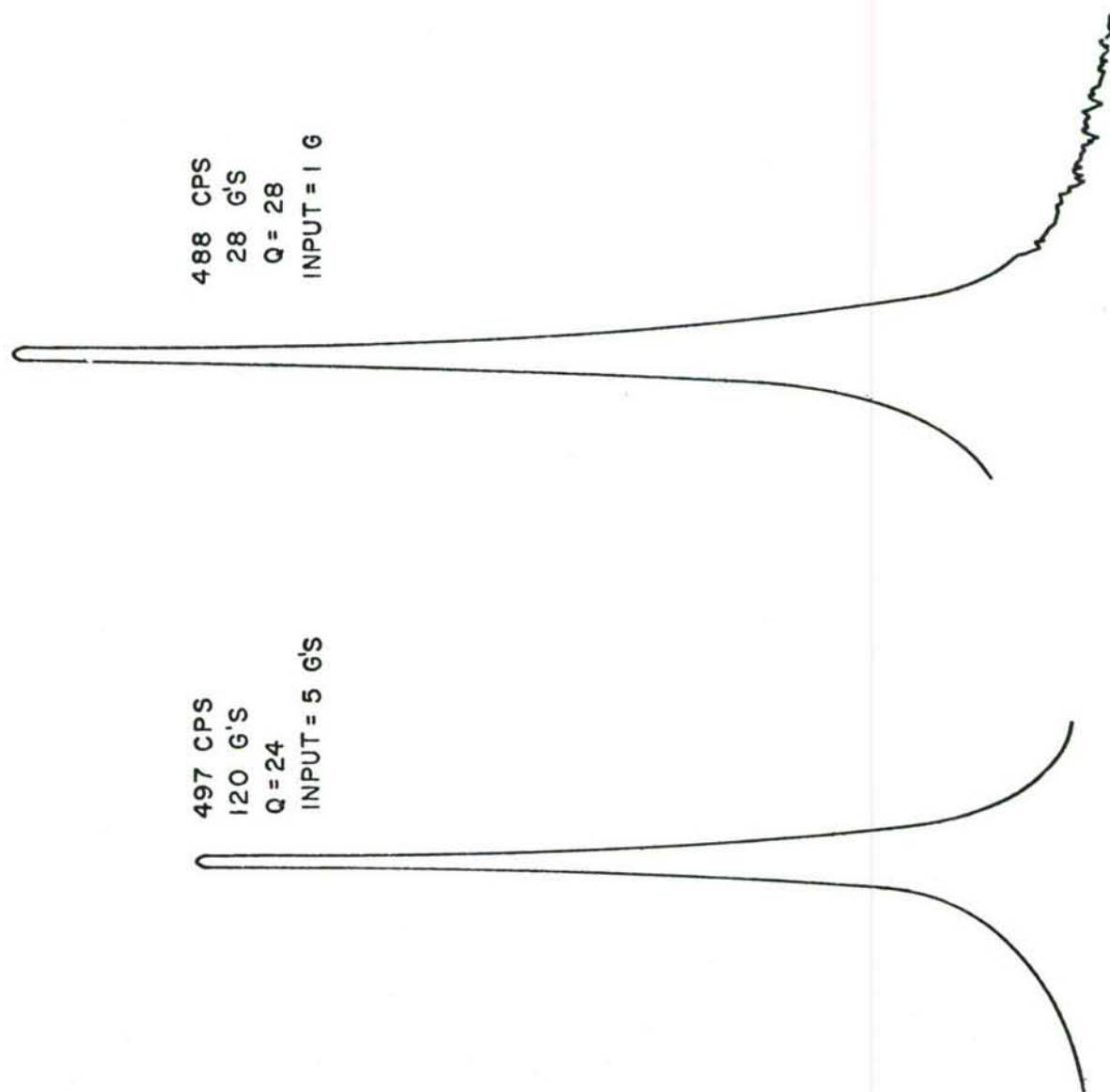


Figure 7. Typical Response Spectra For Undamped Antenna

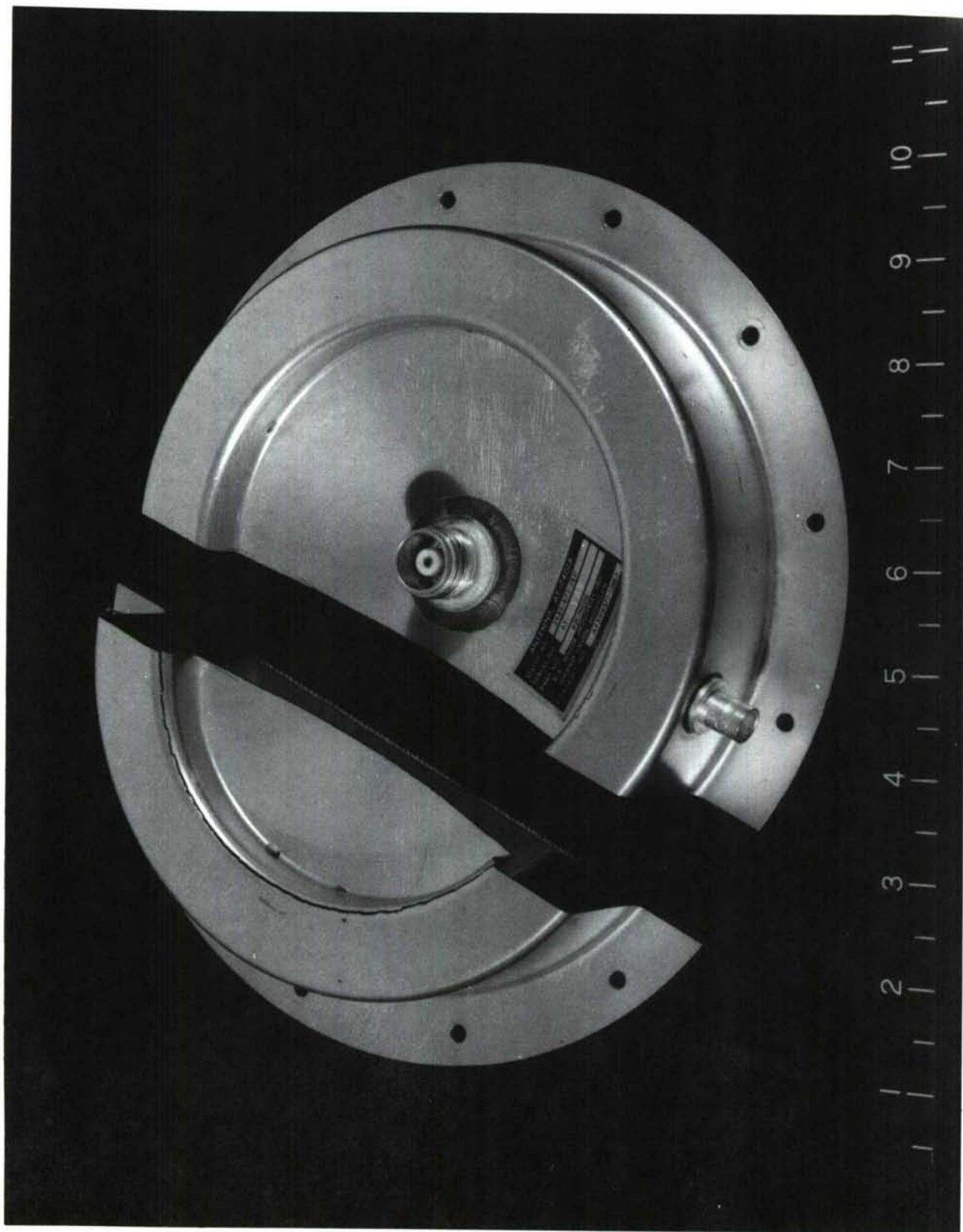


Figure 8. Failure in Antenna

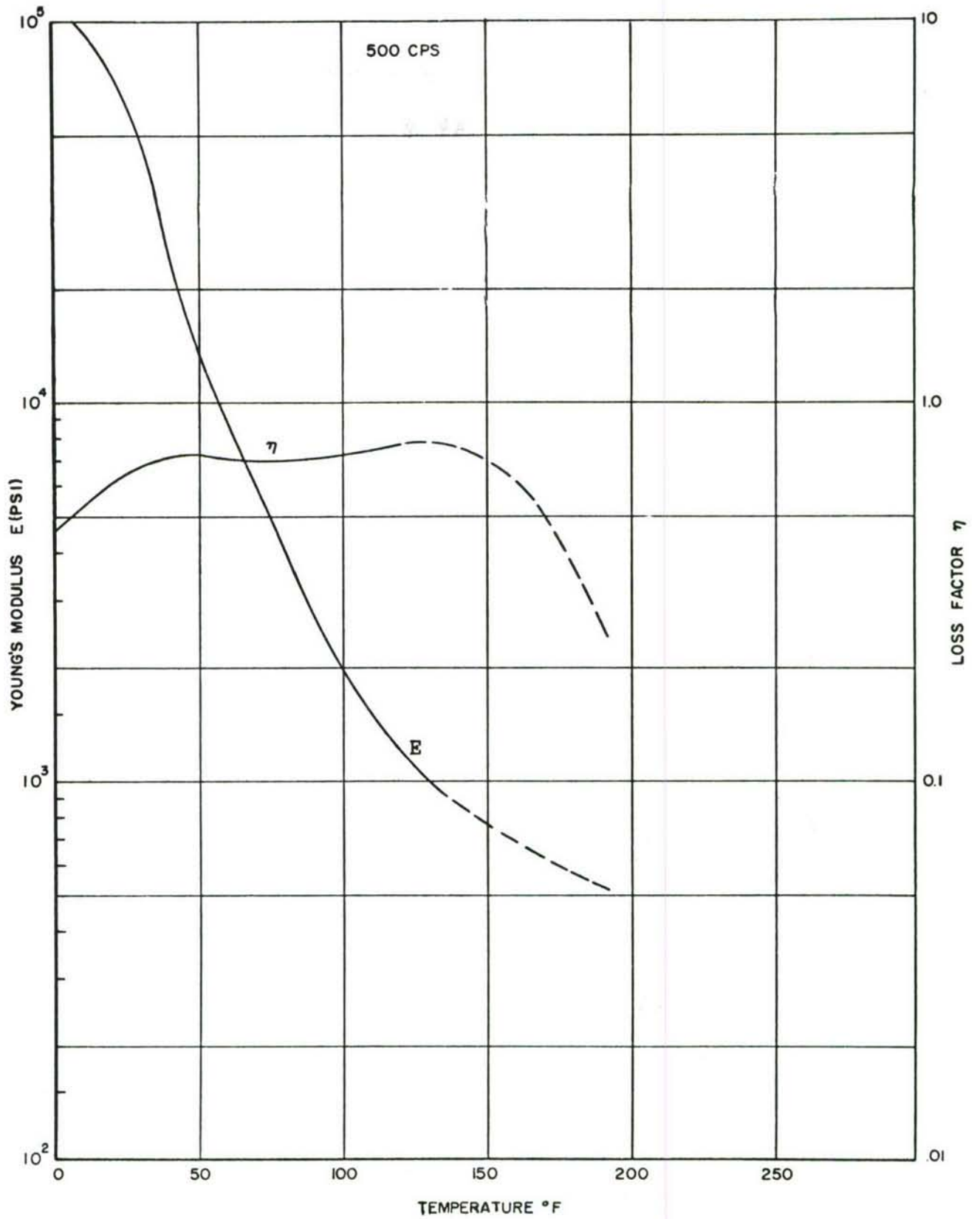


Figure 9. Damping Properties of VPCO-15080 [7]

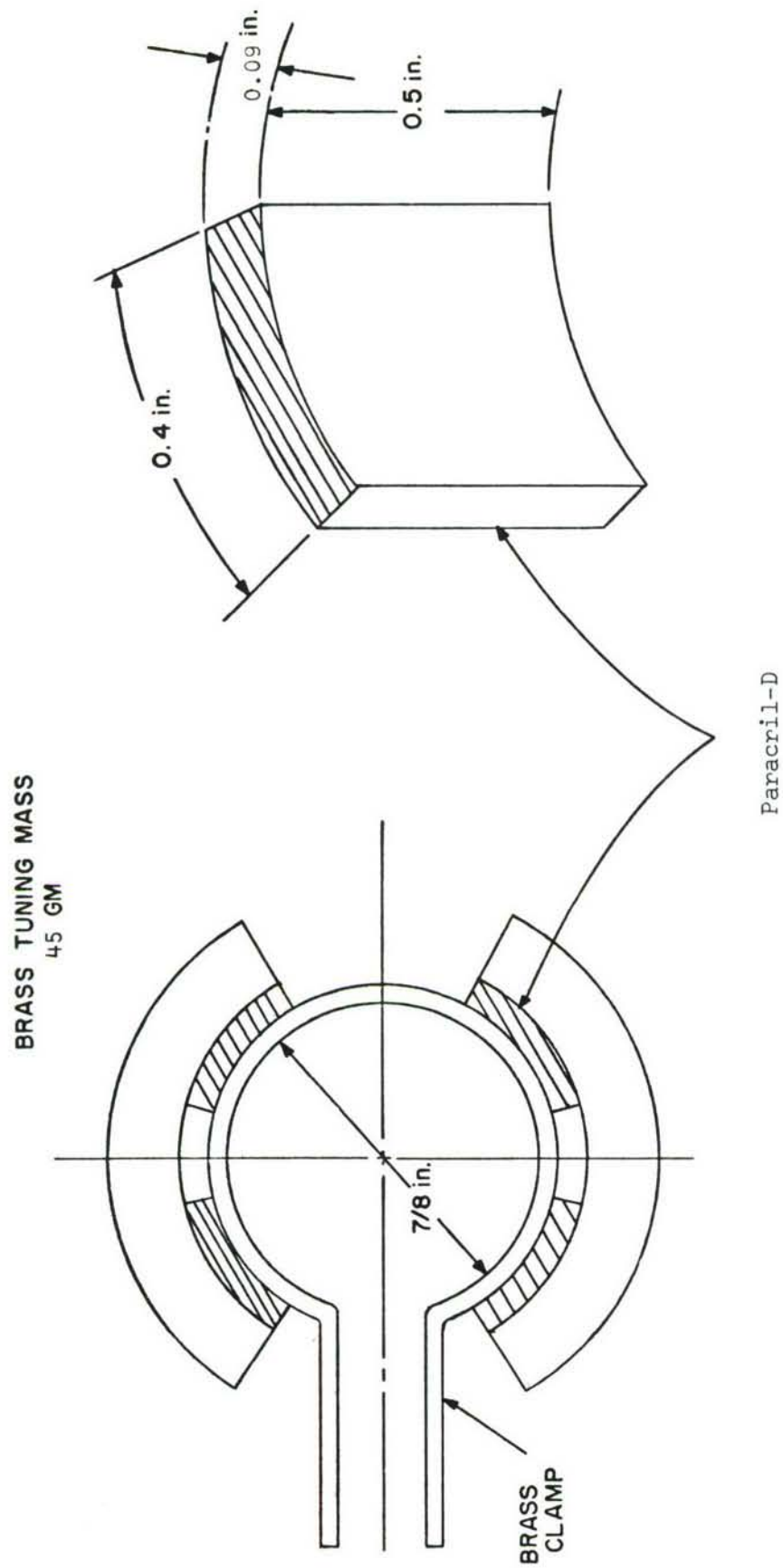


Figure 10. Prototype I Damper Geometry

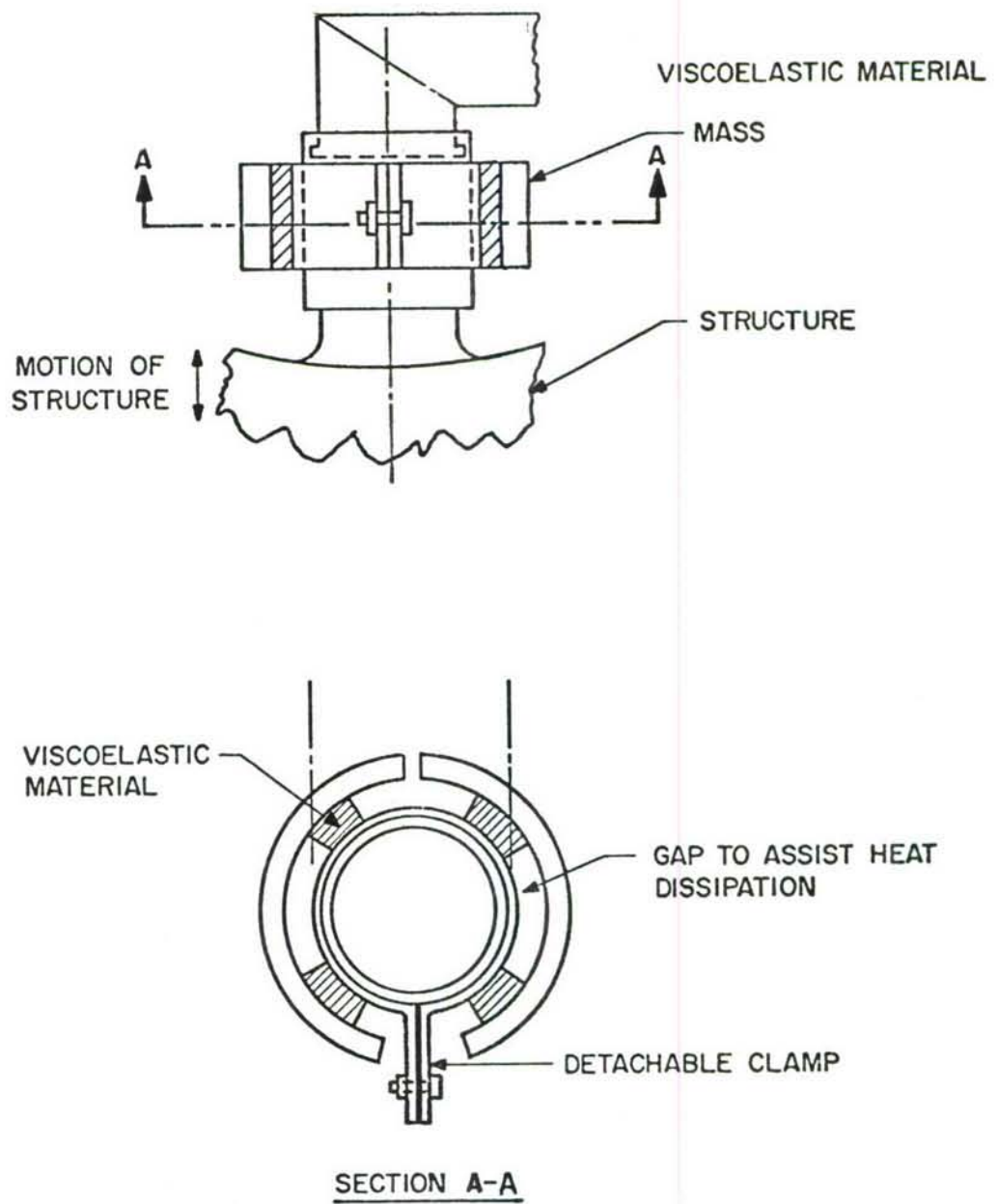
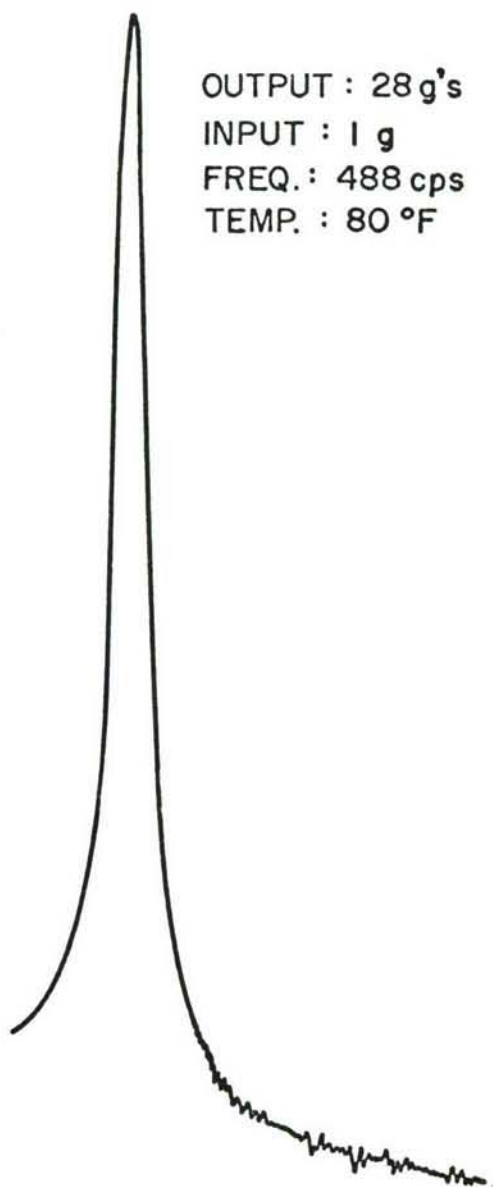


Figure 11. Location of Damper on Connector



OUTPUT : 28 g's
INPUT : 1 g
FREQ. : 488 cps
TEMP. : 80 °F

UNDAMPED ANTENNA

DAMPER MASS : 50 gm
OUTPUT : 10 g's
INPUT : 1 g
FREQ : 439 cps
TEMP : 80 °F
MATERIAL : VPCO - 15080



DAMPED ANTENNA

Figure 12. Typical Response Spectra for Antenna with and without Prototype Damper

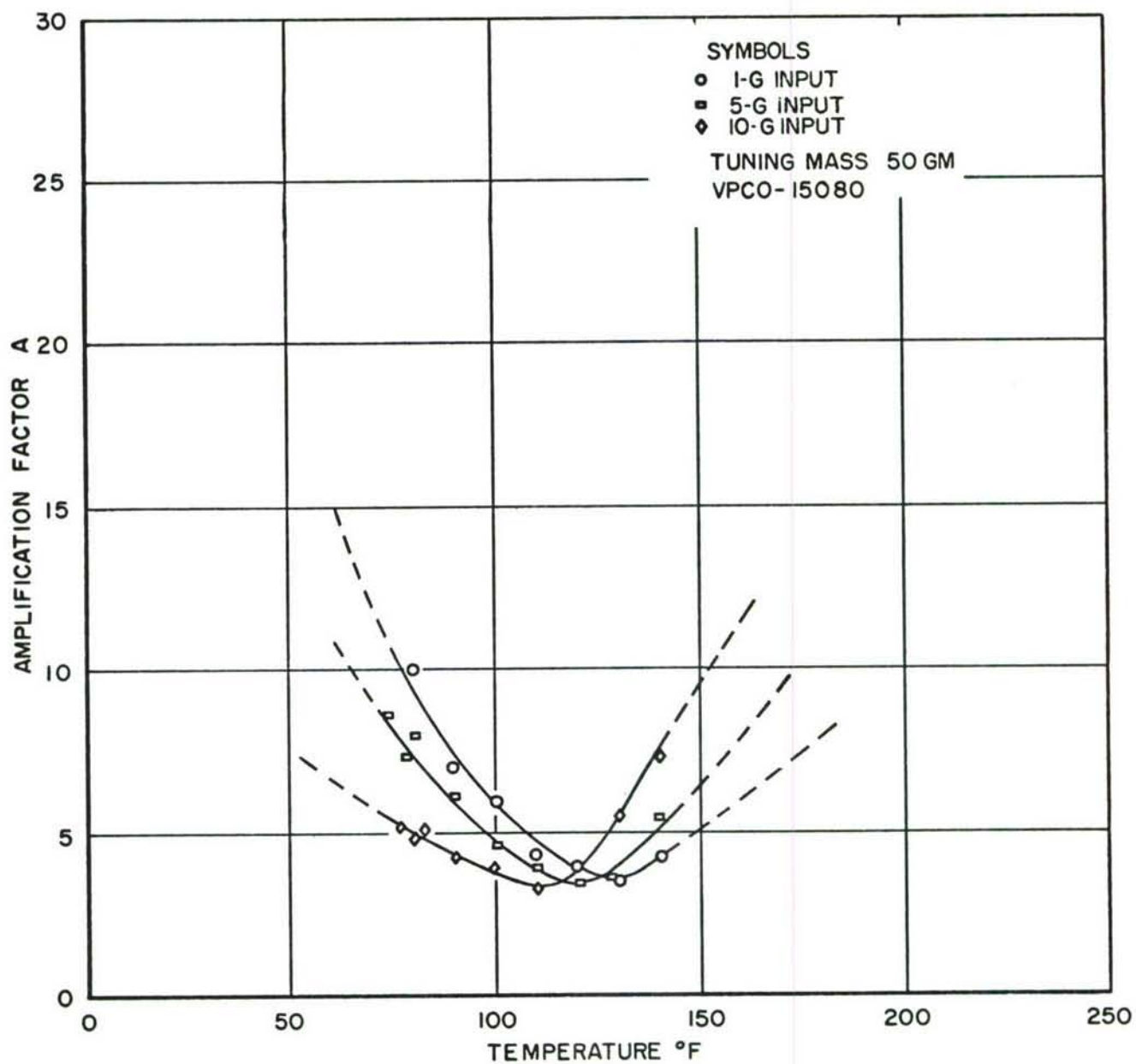


Figure 13. Variation of Amplification Factor A with Temperature for Antenna with Prototype I Attached

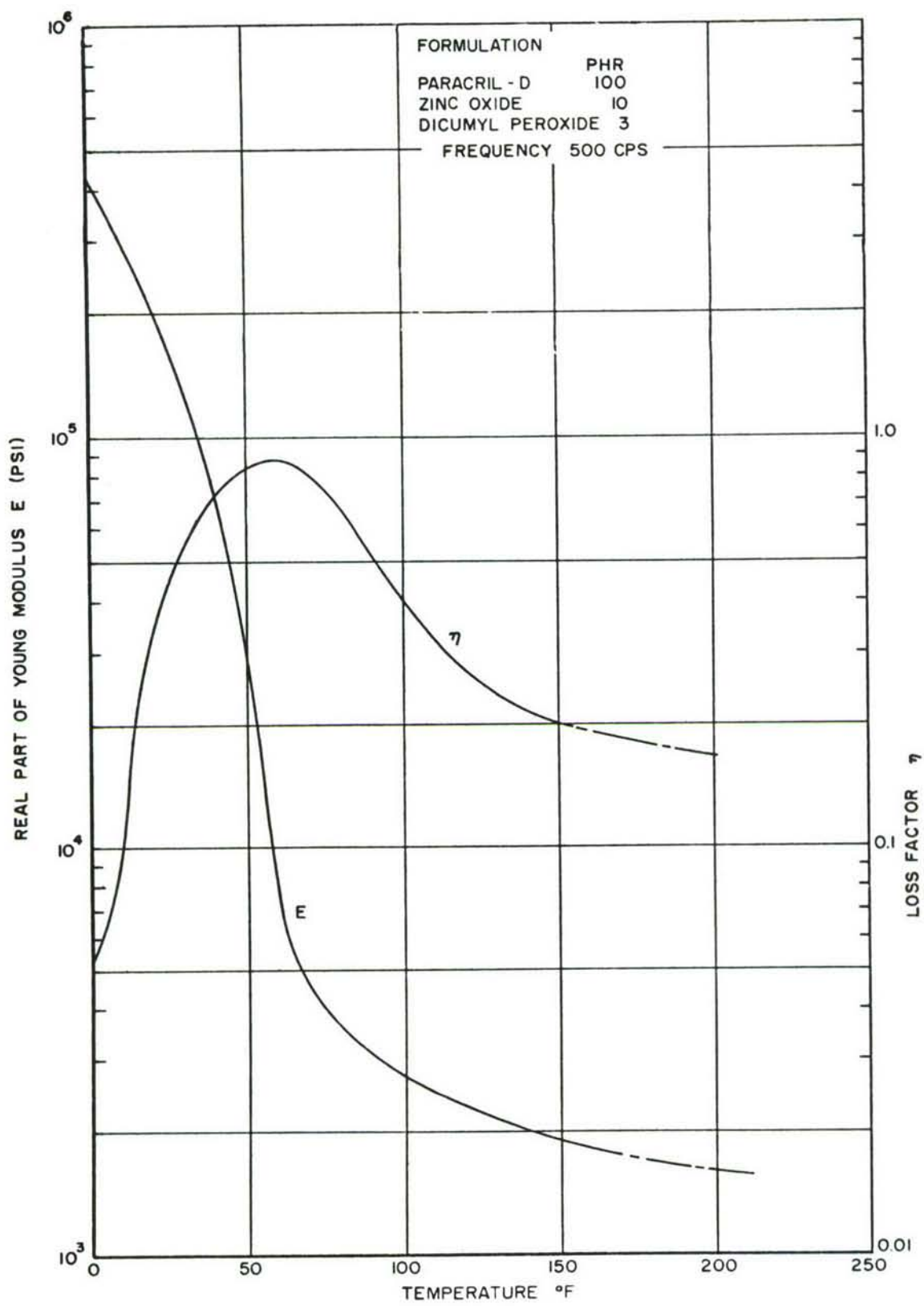


Figure 14. Damping Properties of Paracril-D

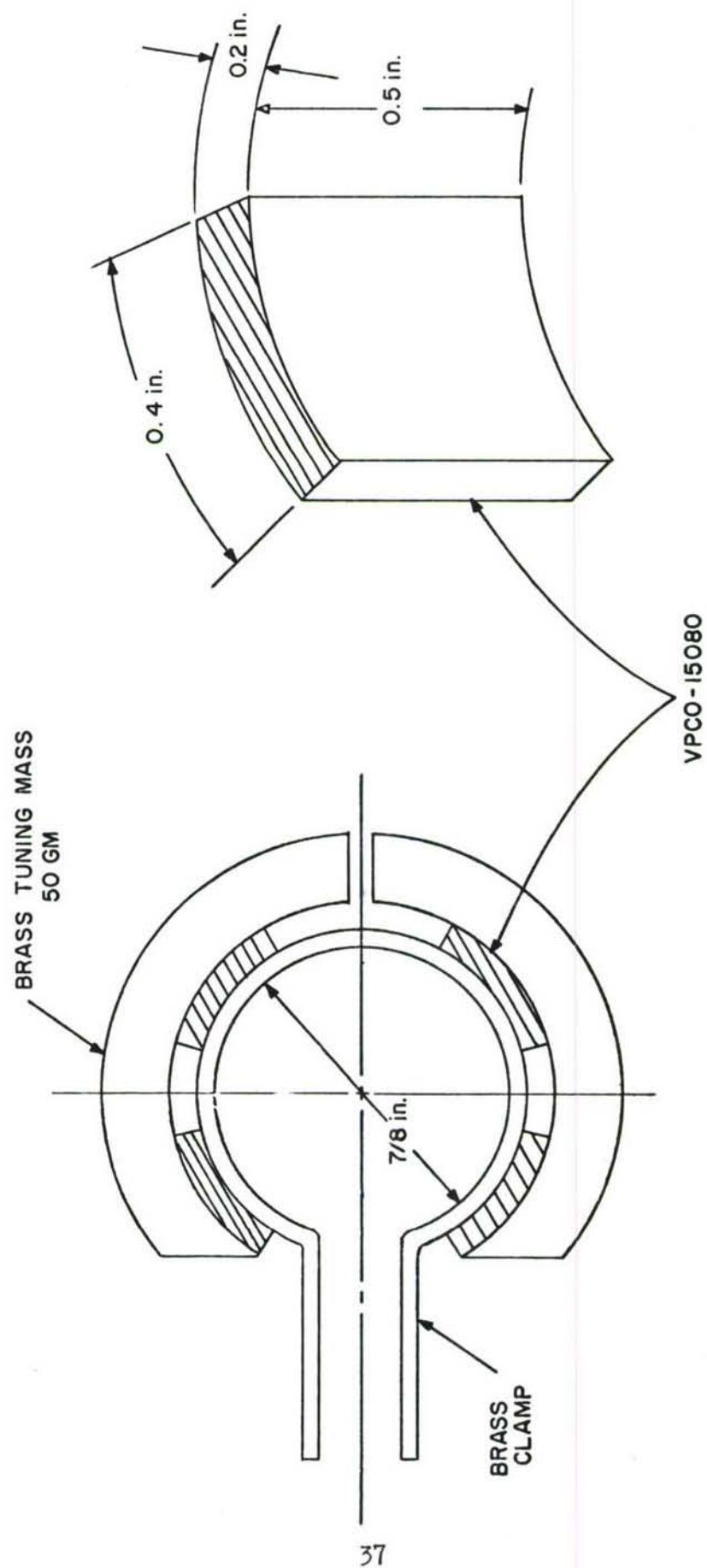


Figure 15. Geometry of Prototype 2

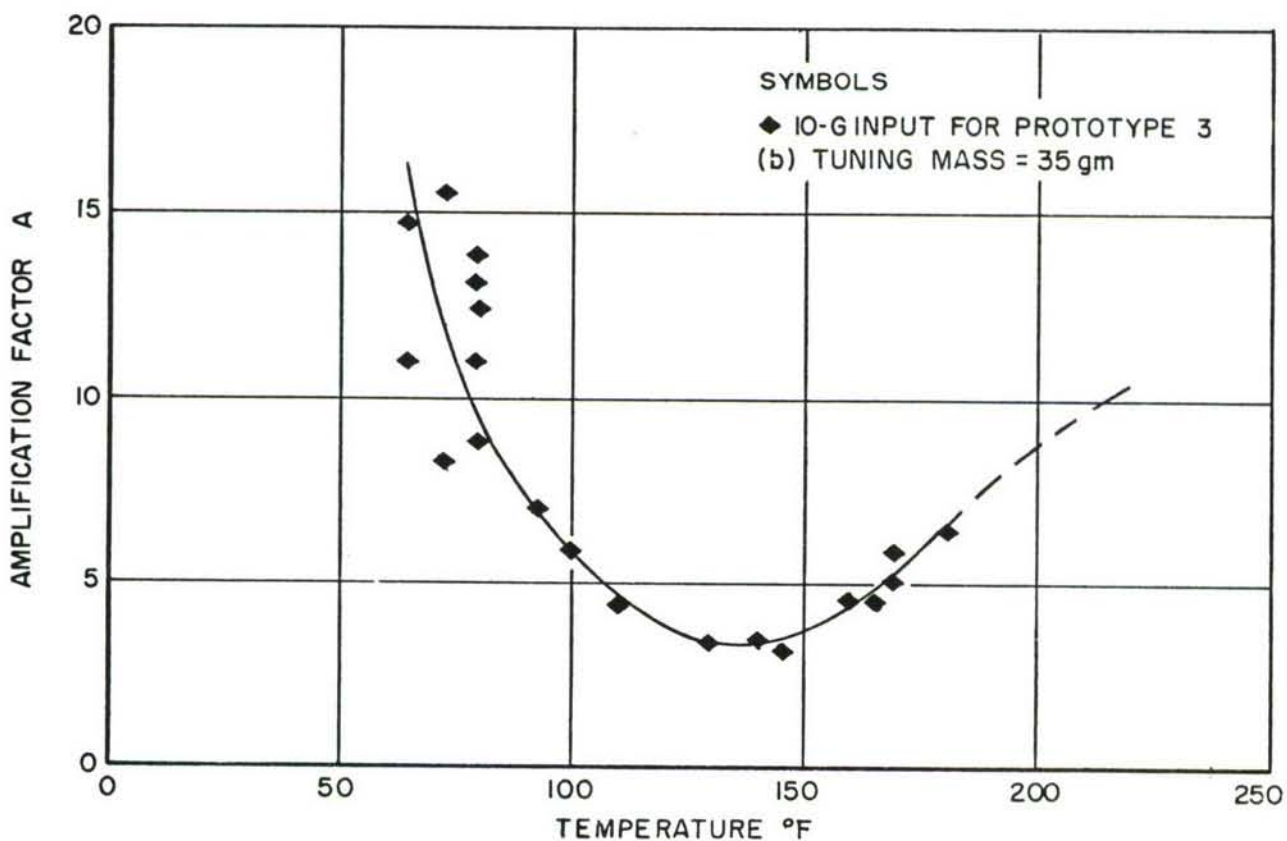
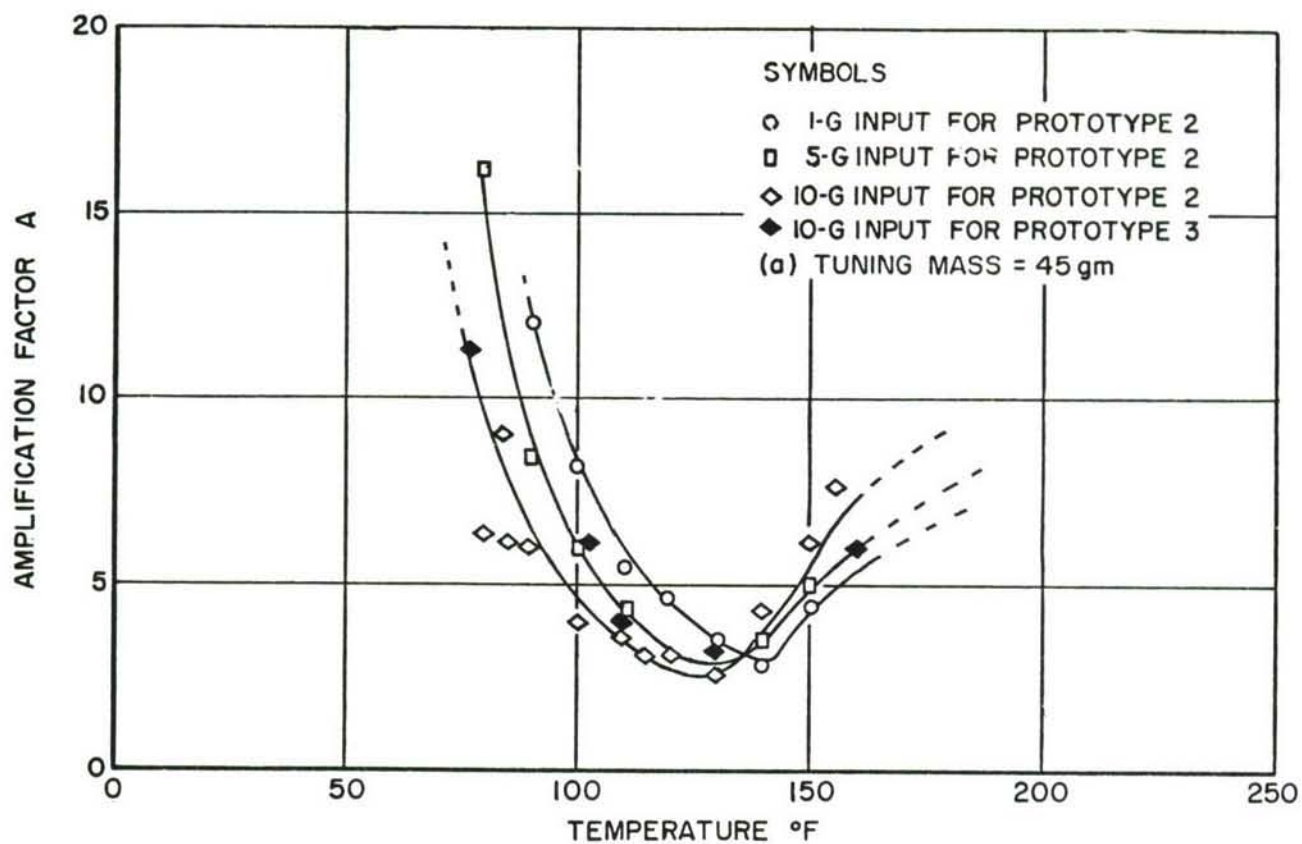


Figure 16. Variation of Amplification Factor A with Temperature for Antenna with Prototypes 2 and 3 Attached

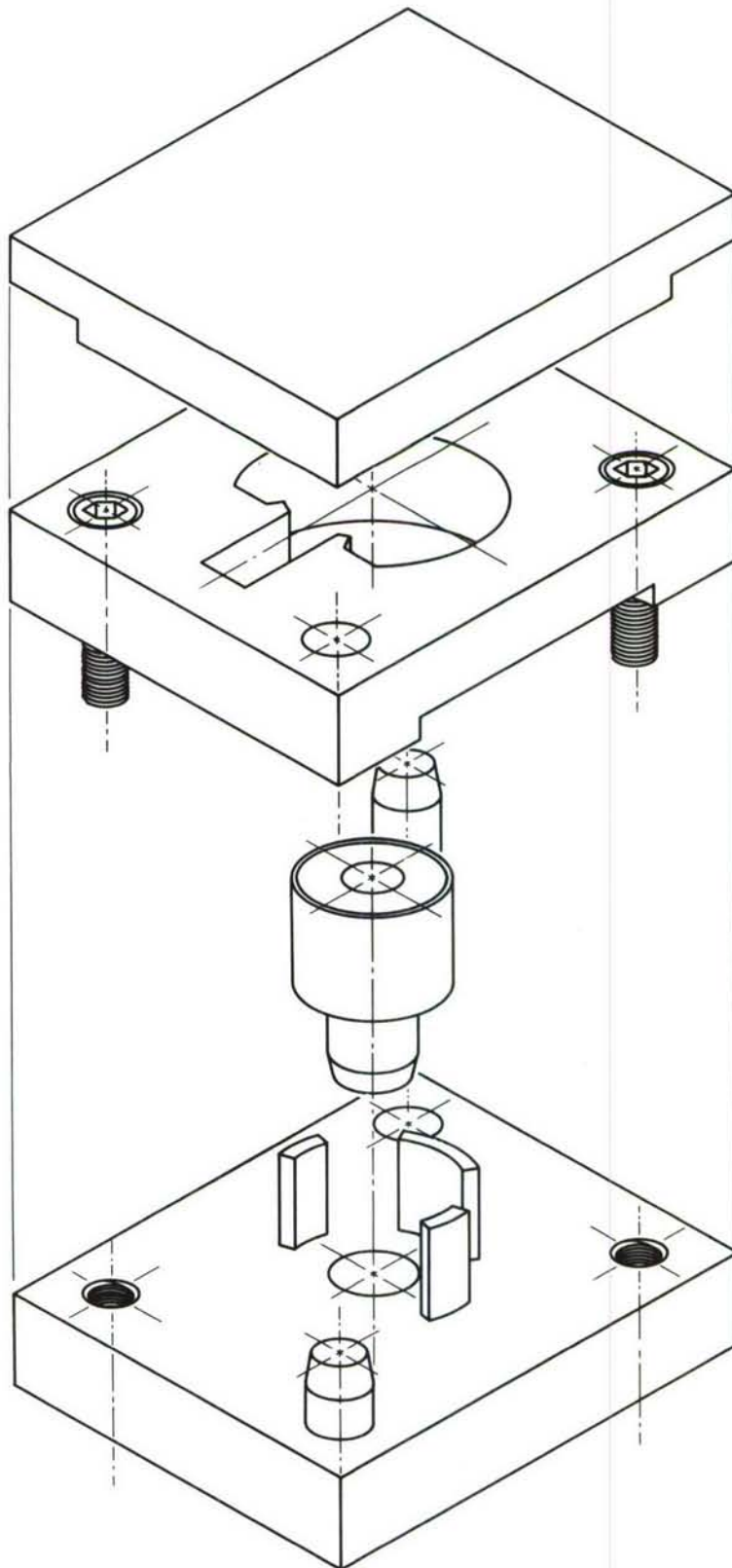


Figure 17. Exploded View of Mold

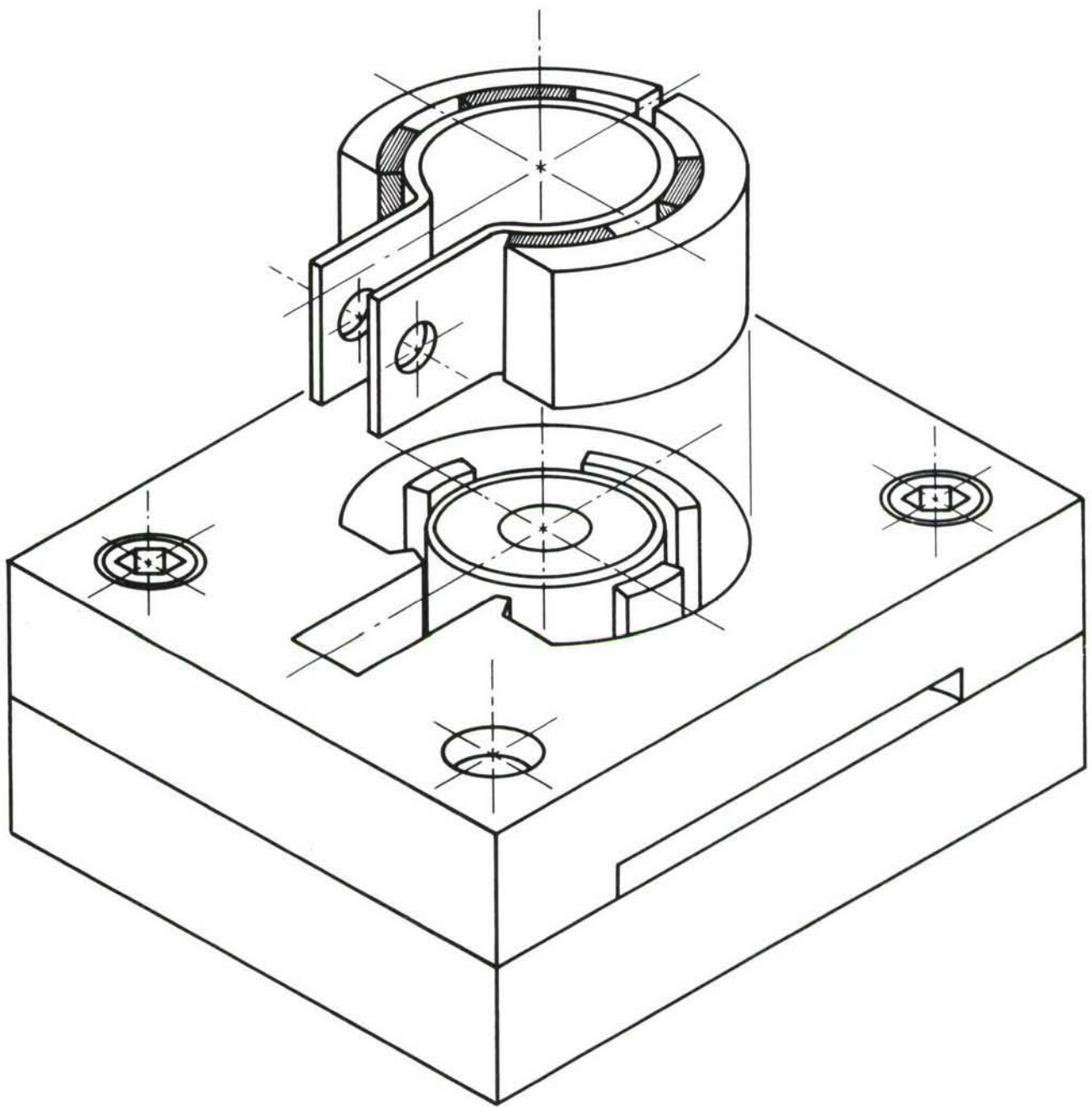


Figure 18. Layout of Damper in Mold

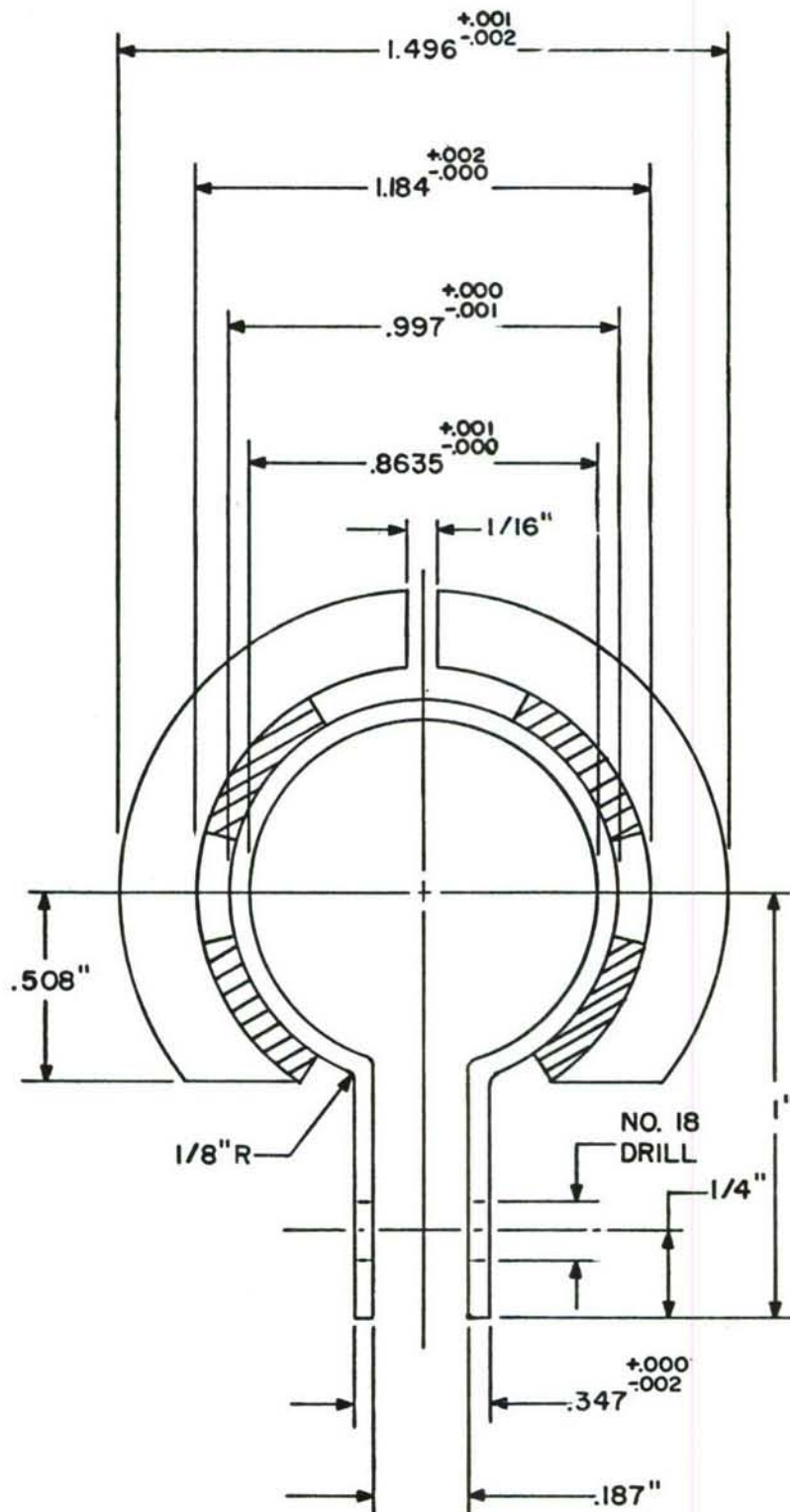


Figure 19. Geometry of Prototype 2

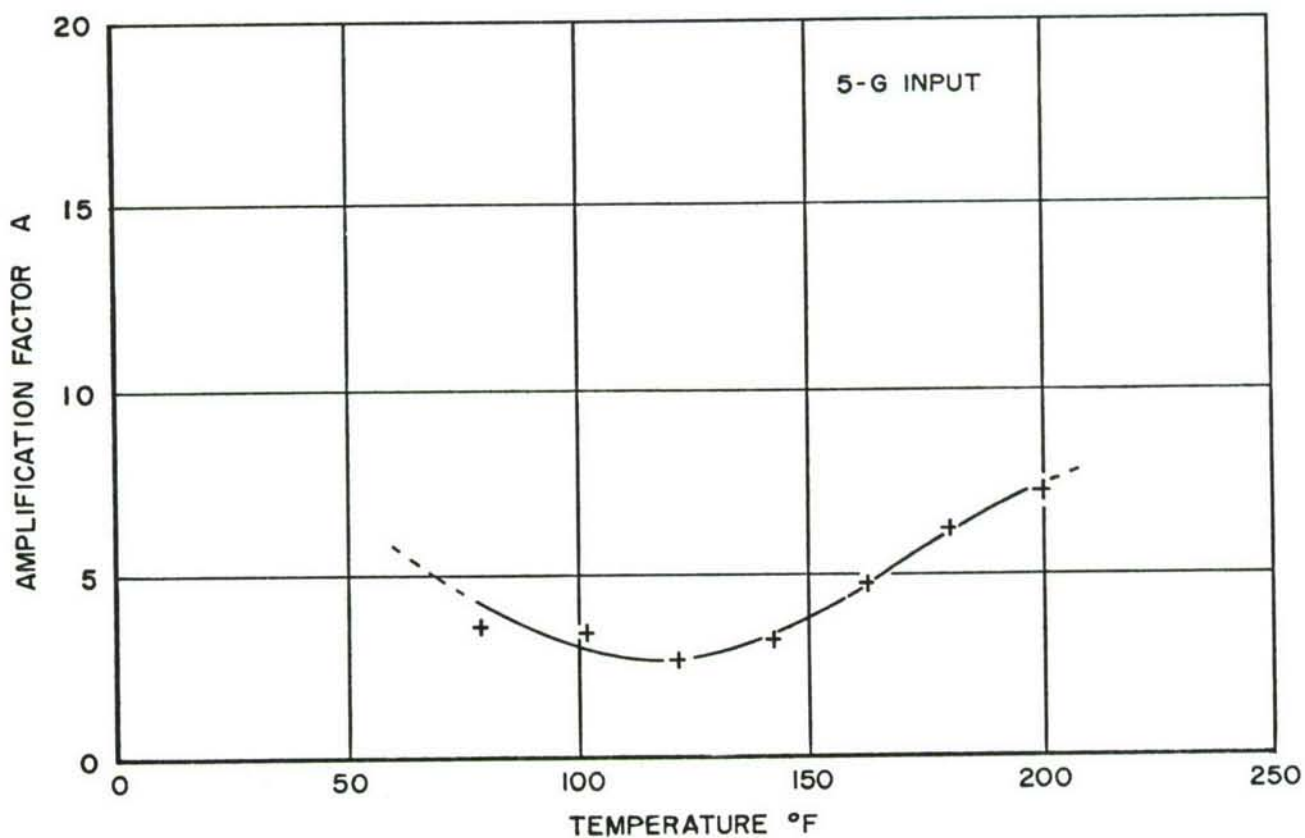
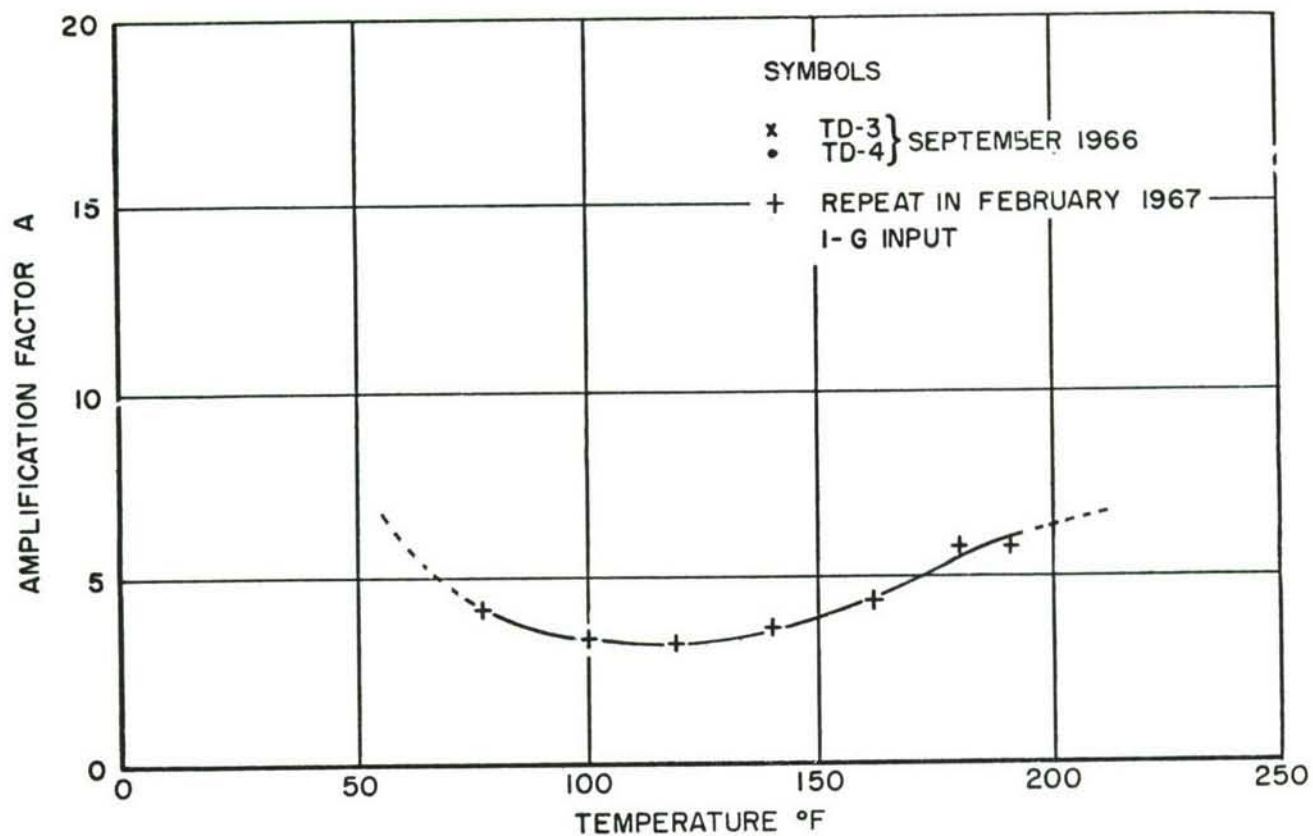


Figure 20. Variation of Amplification Factor A with Temperature for Antenna with Prototype 4 Attached (1 and 5-g input)

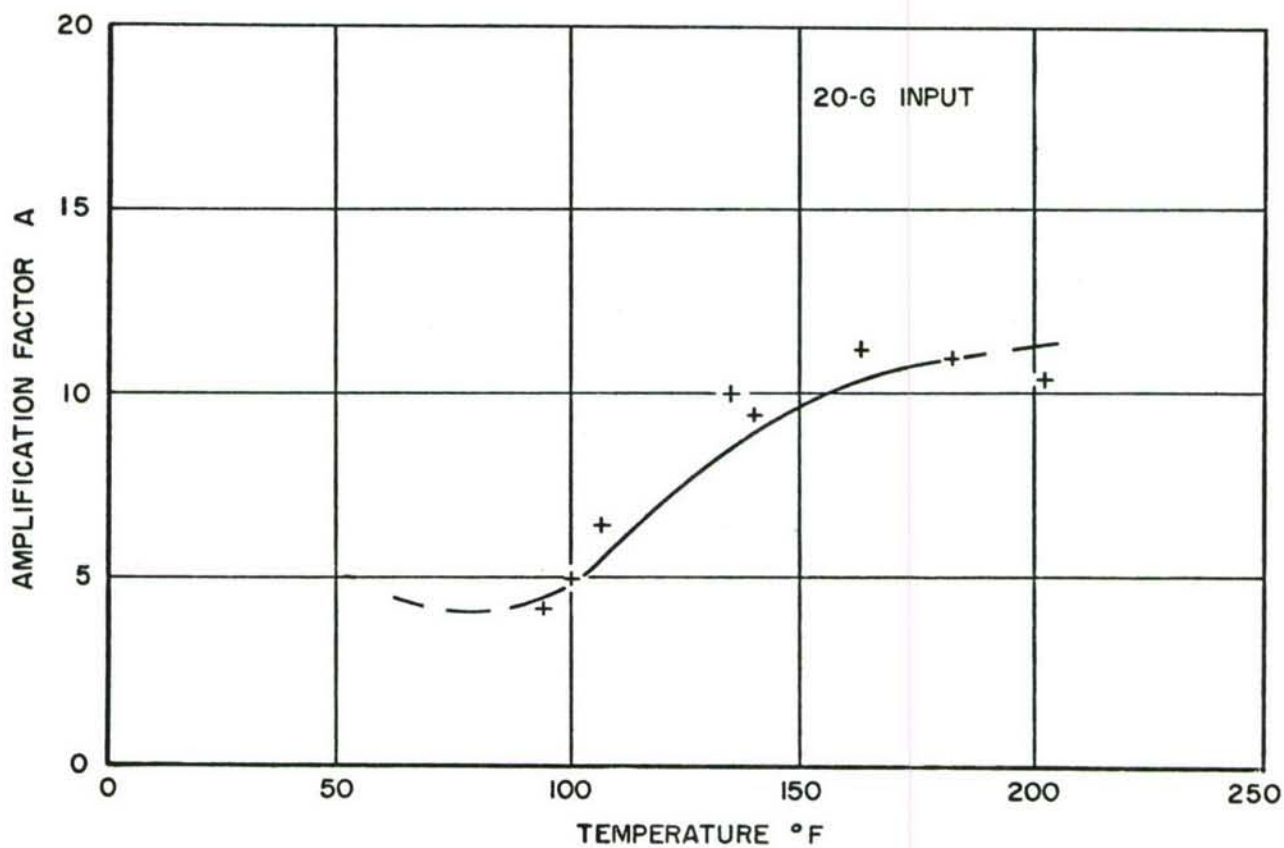
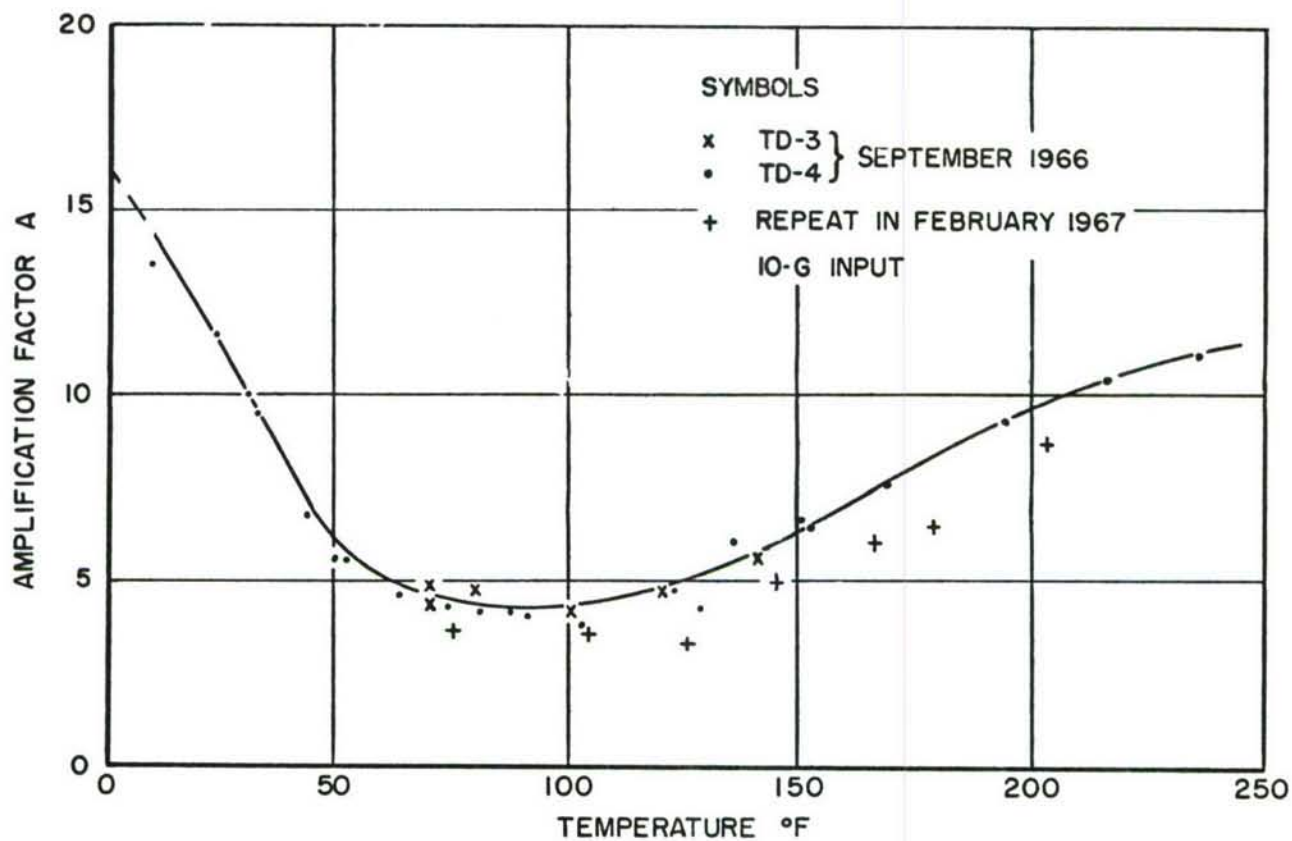


Figure 21. Variation of Amplification Factor A with Temperature for Antenna with Prototype 4 Attached (10 and 20-g input)

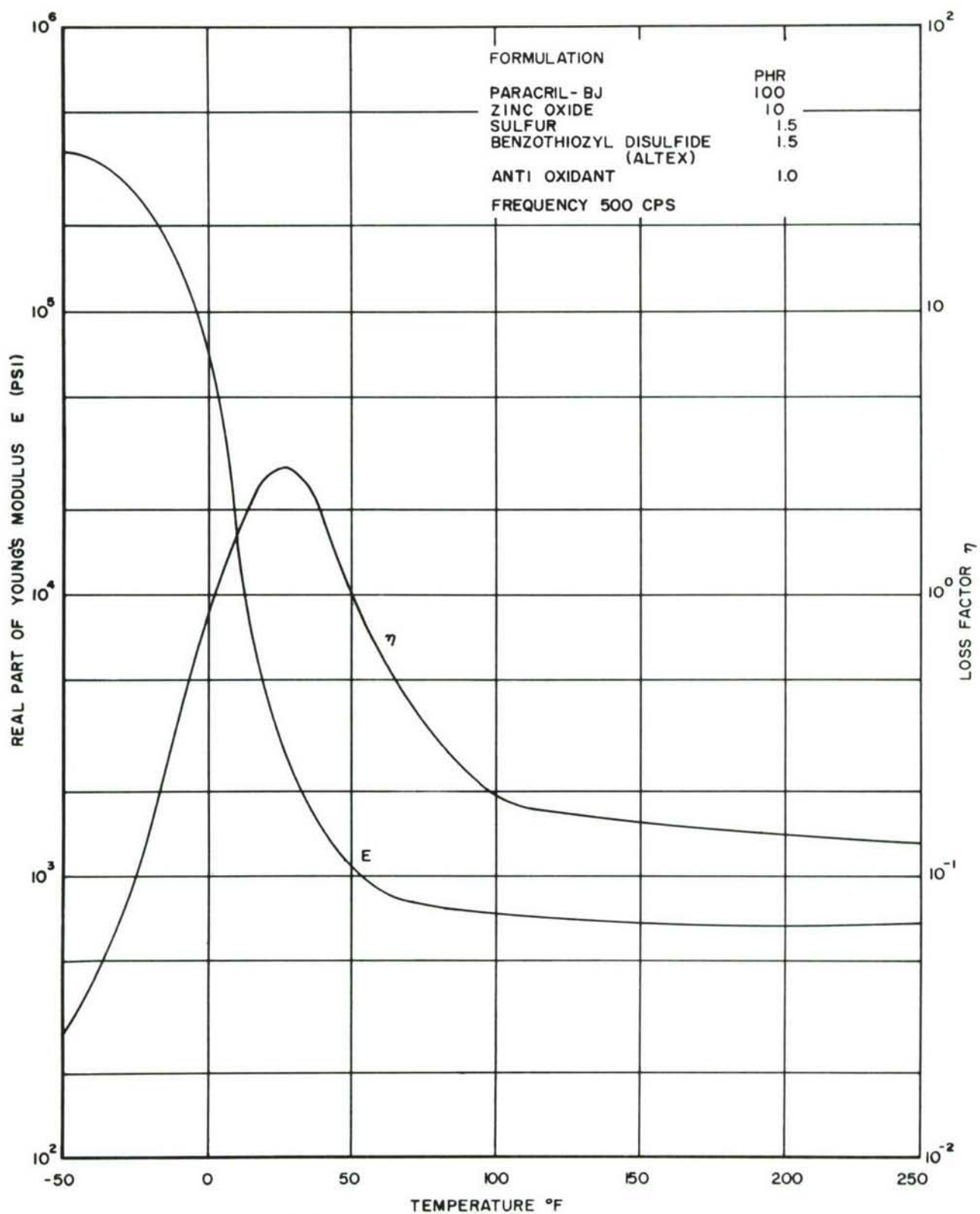


Figure 22. Damping Properties of Paracril-BJ

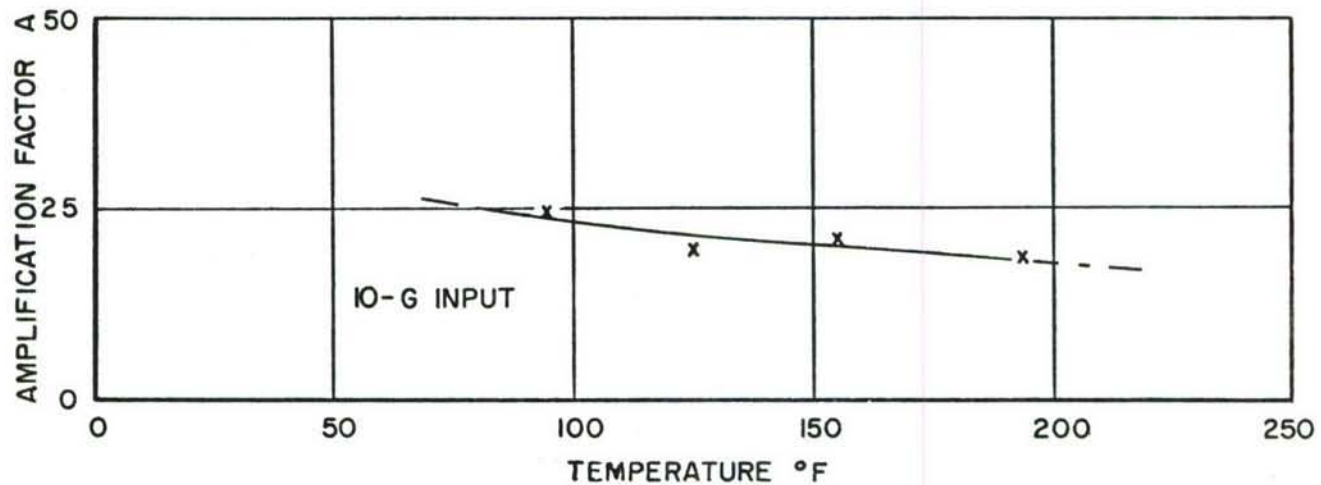
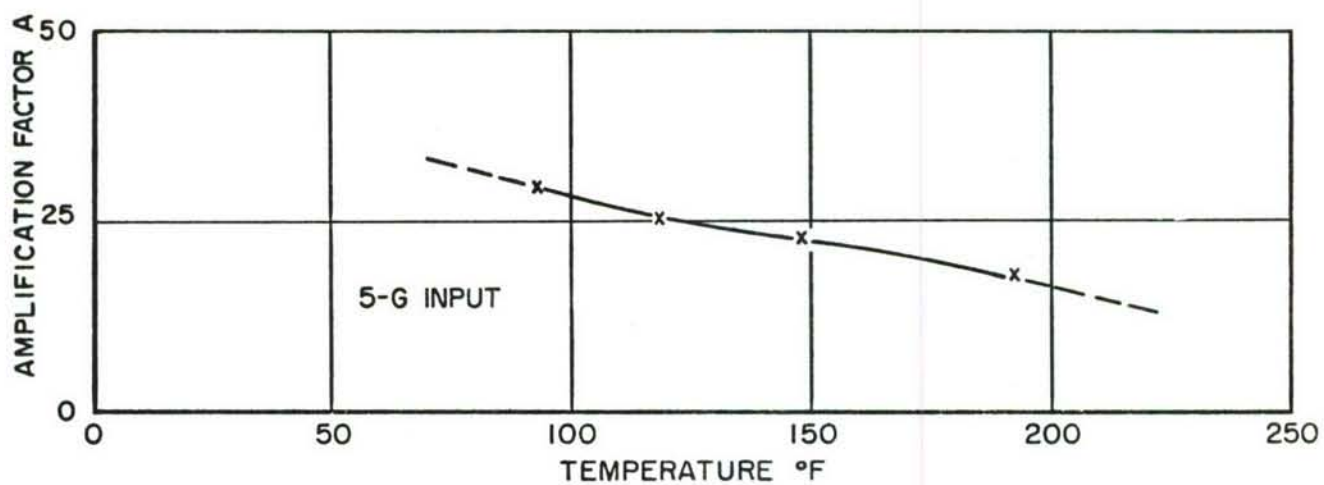
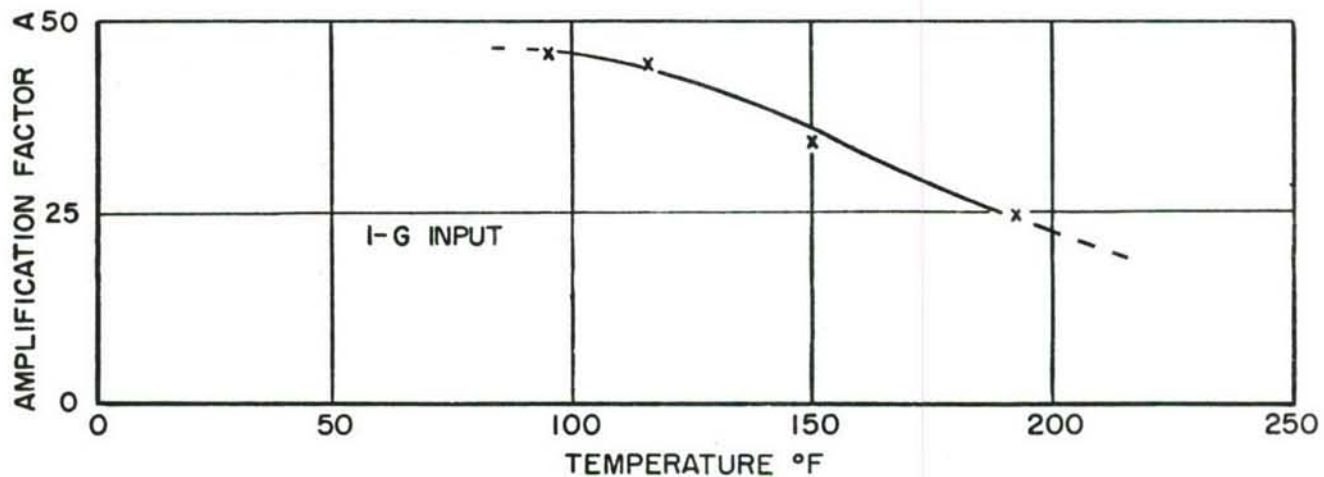


Figure 23. Variation of Amplification Factor A with Temperature for Antenna with Prototype 5 Attached

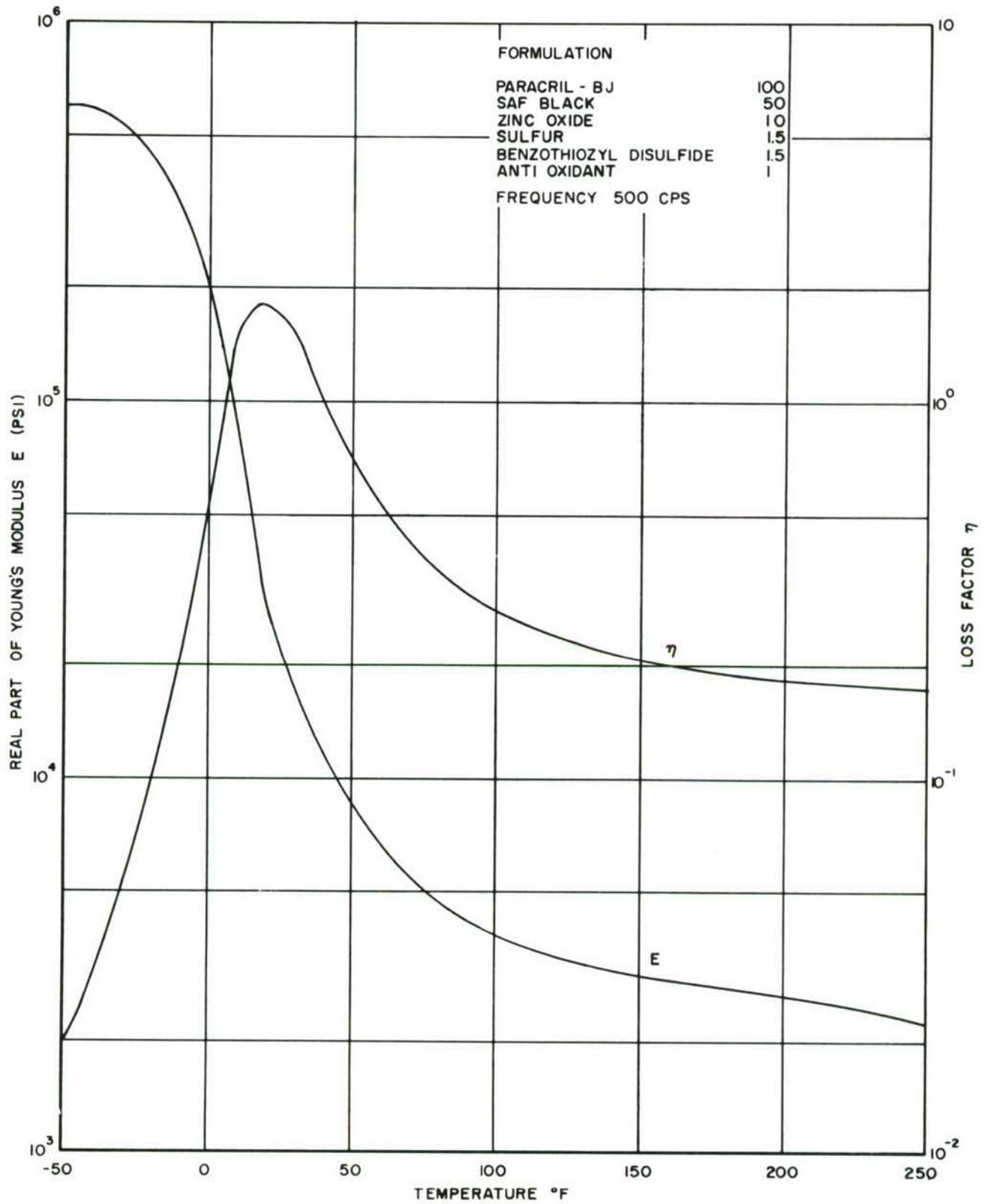


Figure 24. Damping Properties of Paracril-BJ with 50 PHR Carbon

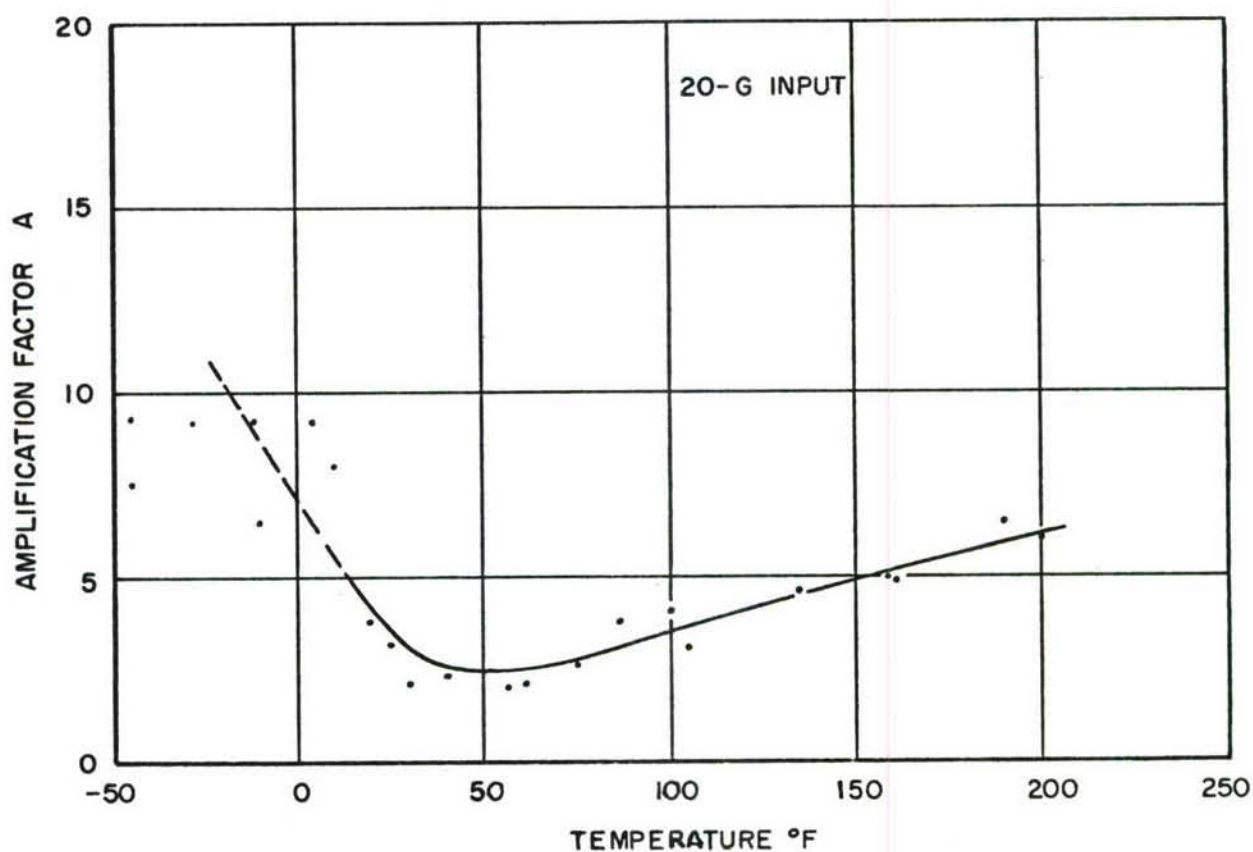
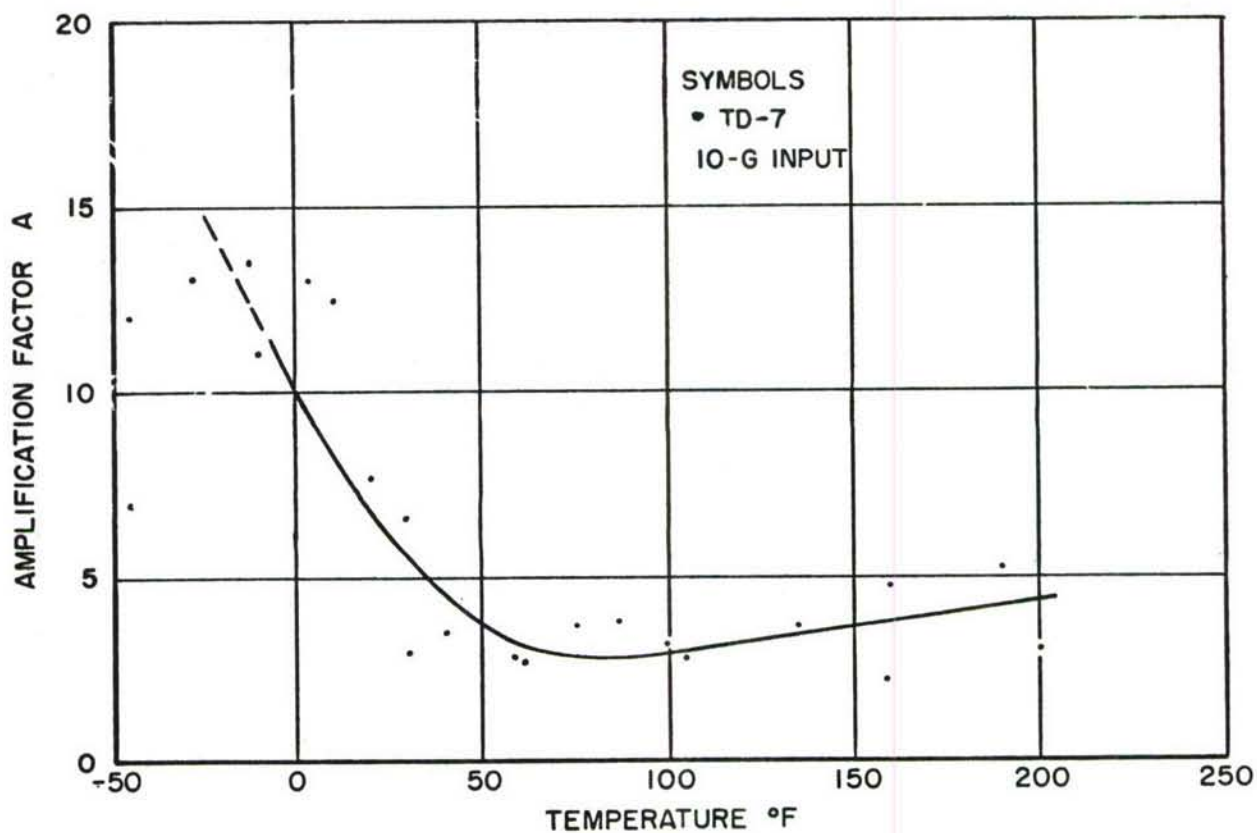


Figure 25. Variation of Amplification Factor A with Temperature for Antenna with Prototype 6 Attached

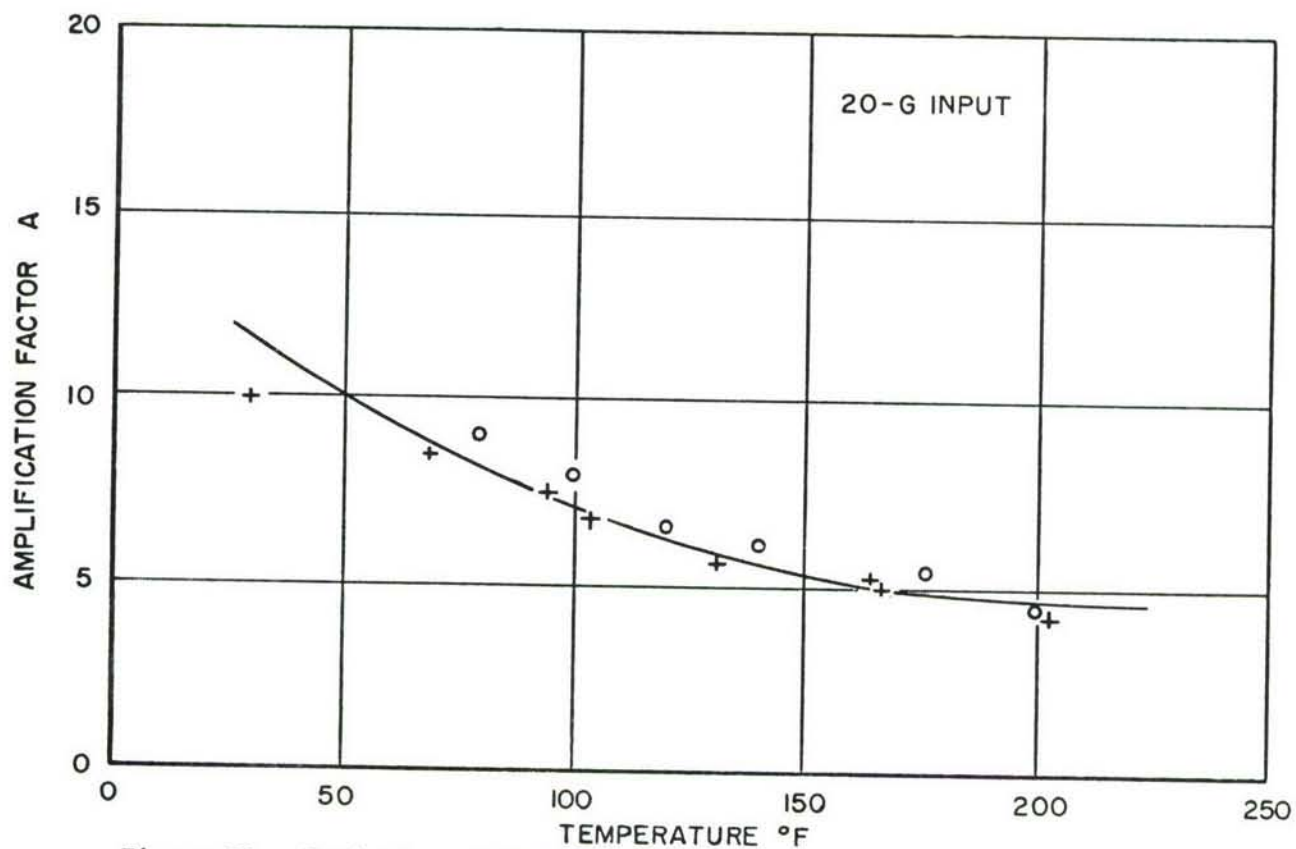
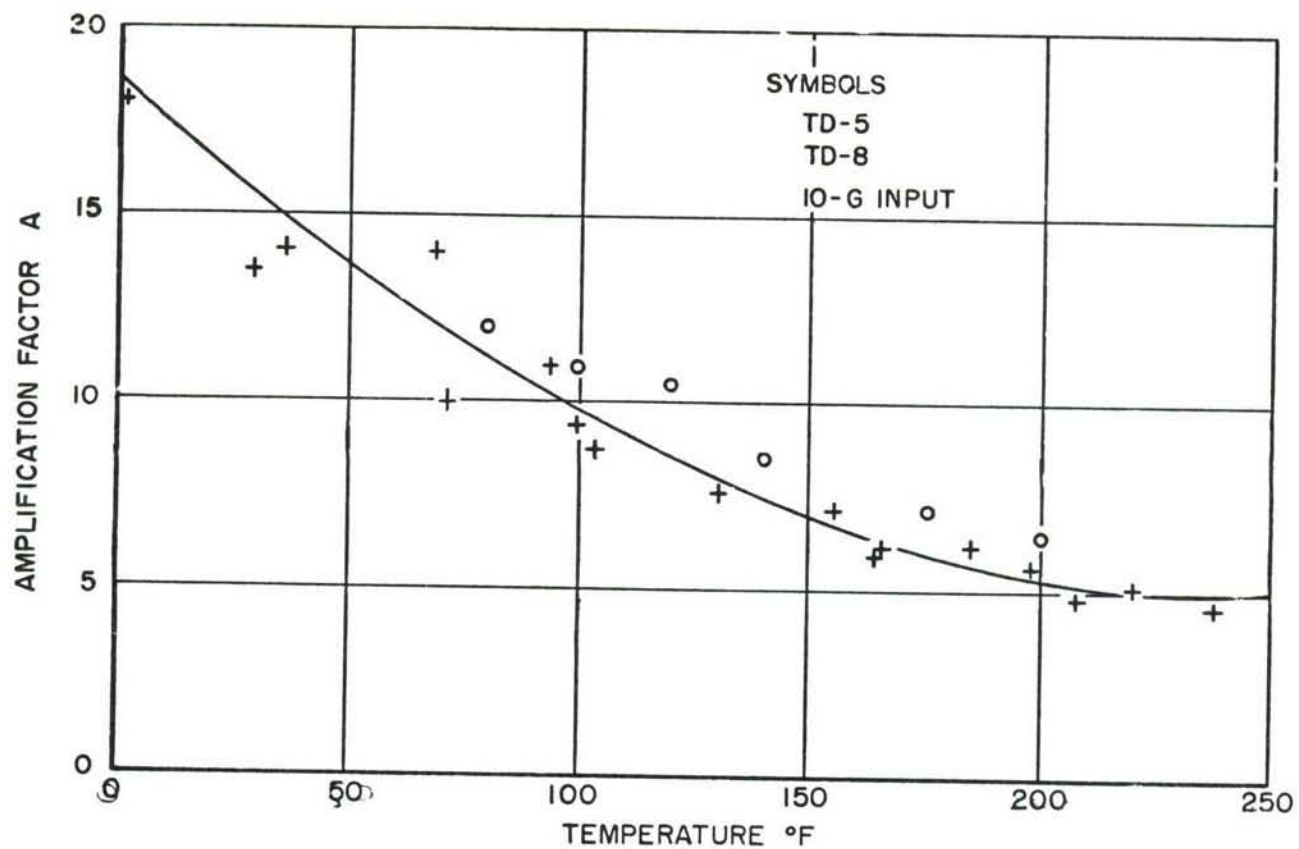


Figure 26. Variation of Amplification Factor A with Temperature for Antenna with Prototype 7 Attached

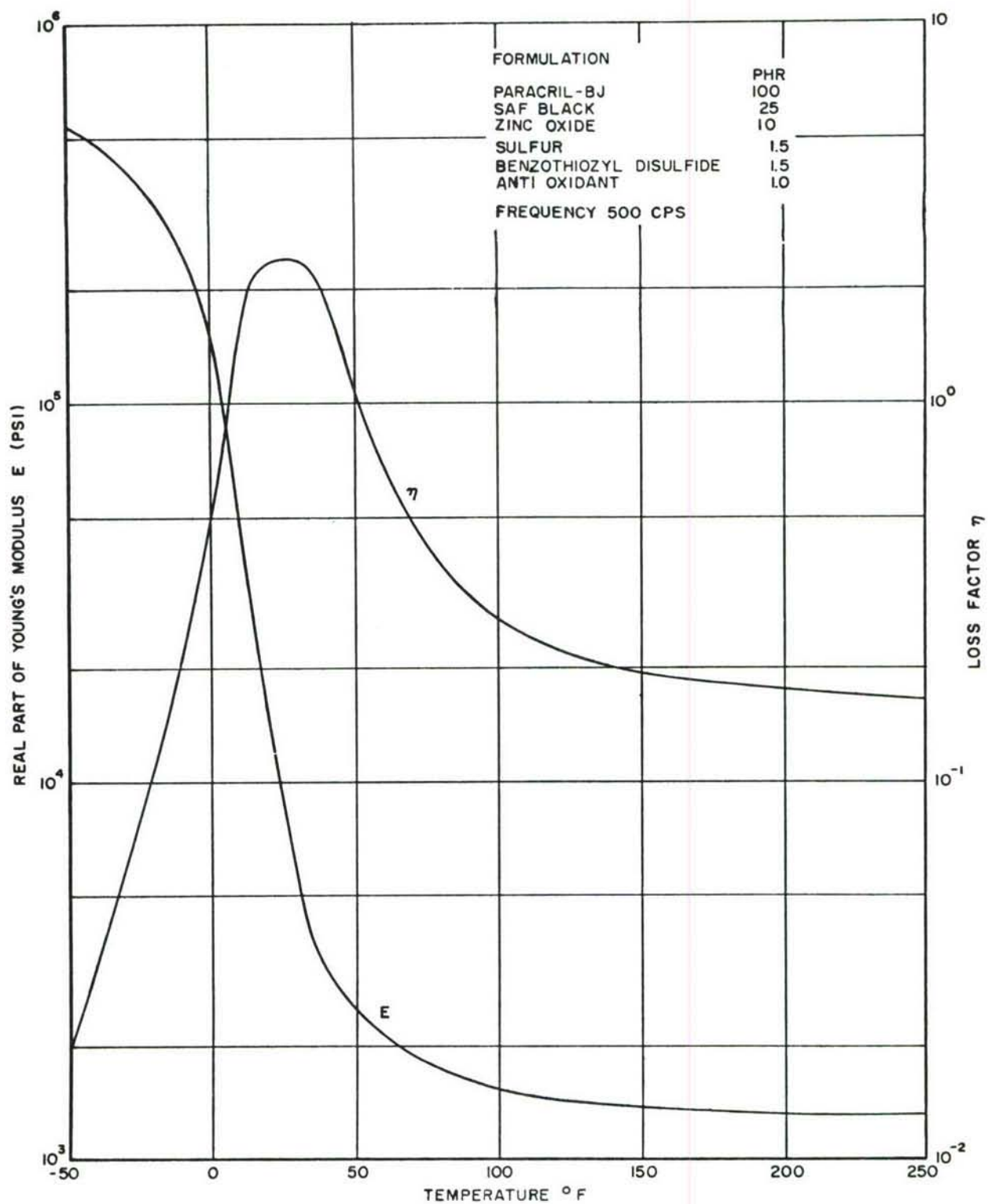


Figure 27. Damping Properties of Paracril-BJ with 25 PHR Carbon

MATERIAL: QQ-B-626 BRASS

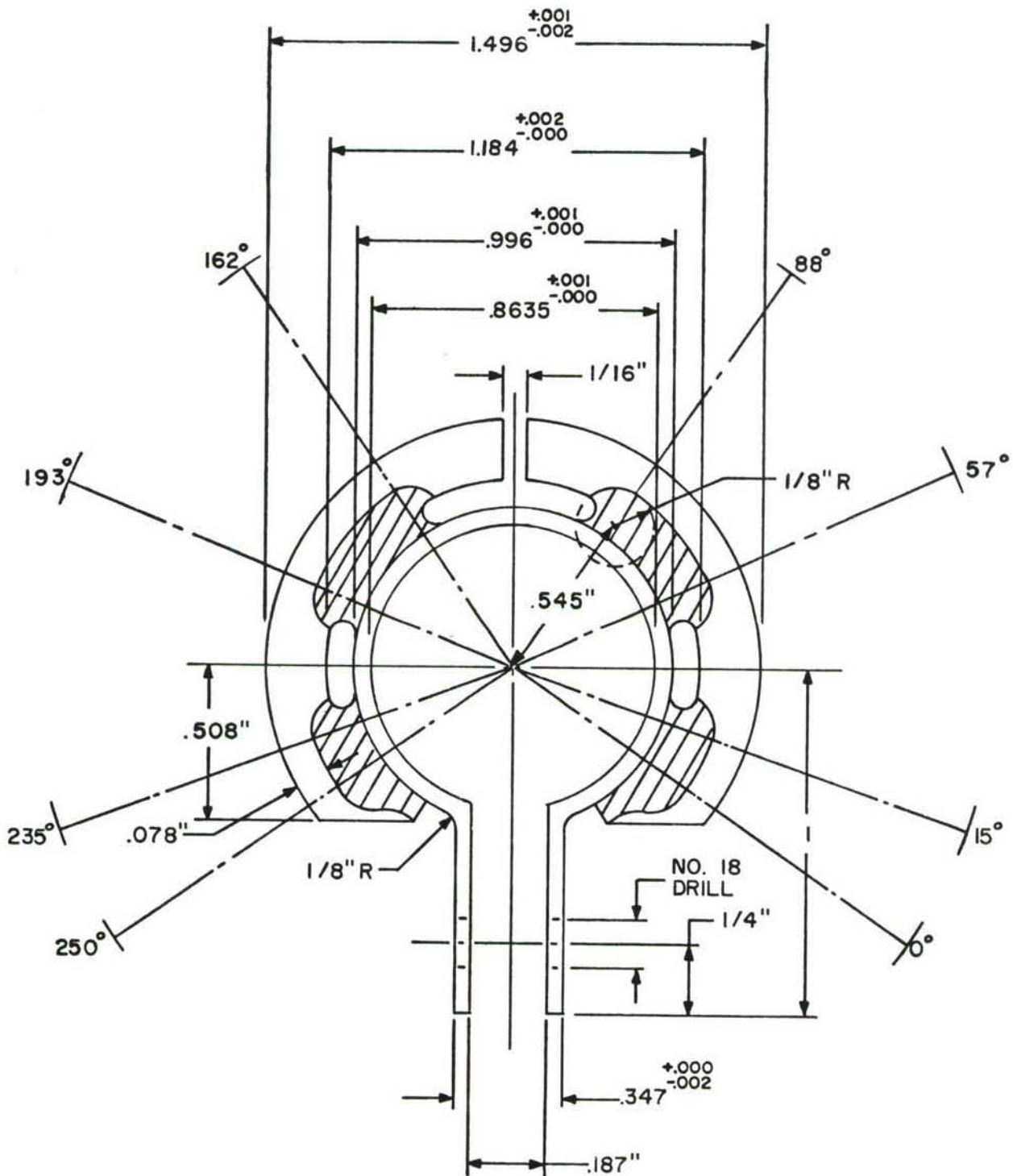


Figure 28. Geometry of Prototype 8 and Subsequent Dampers

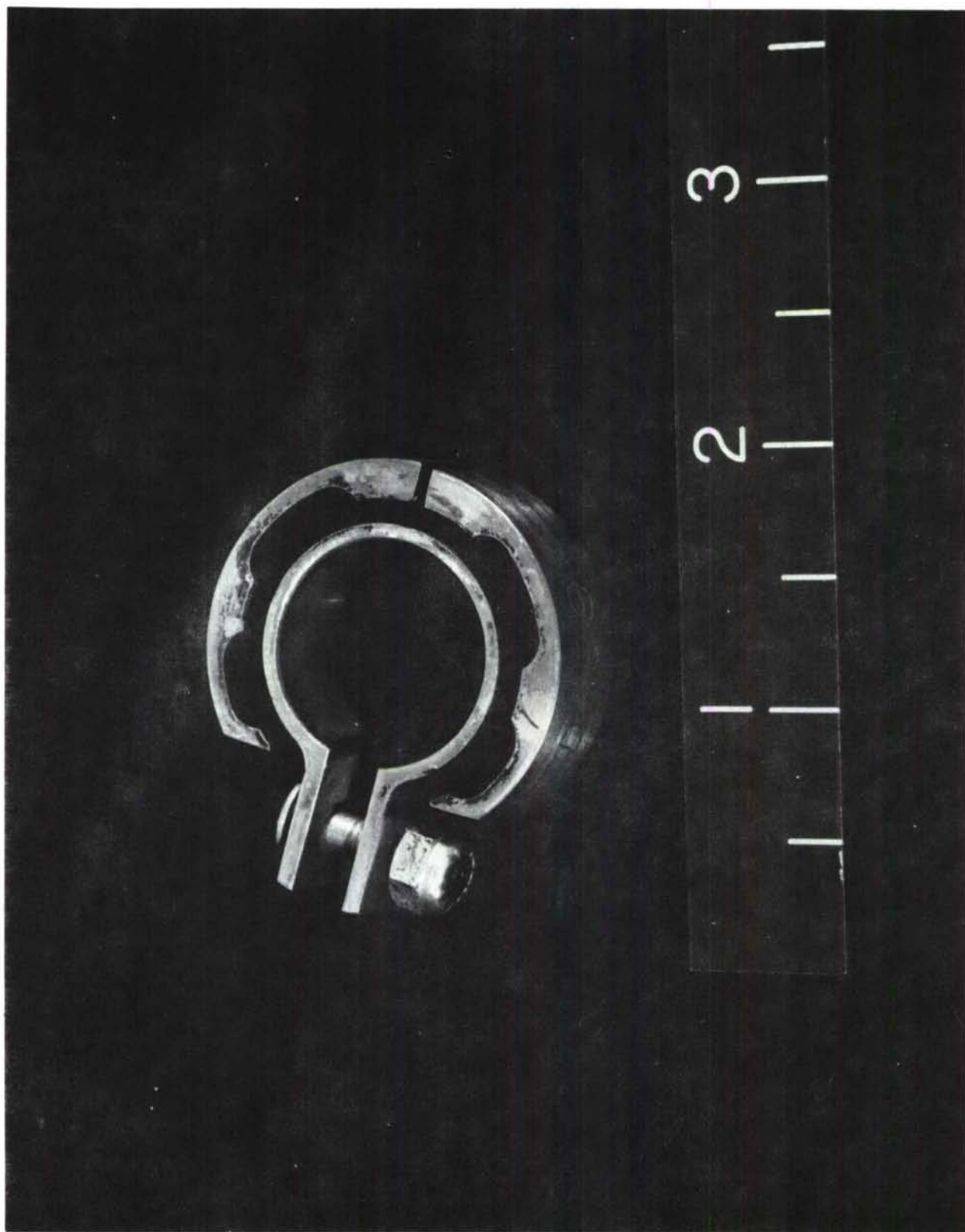


Figure 29. Production Damper

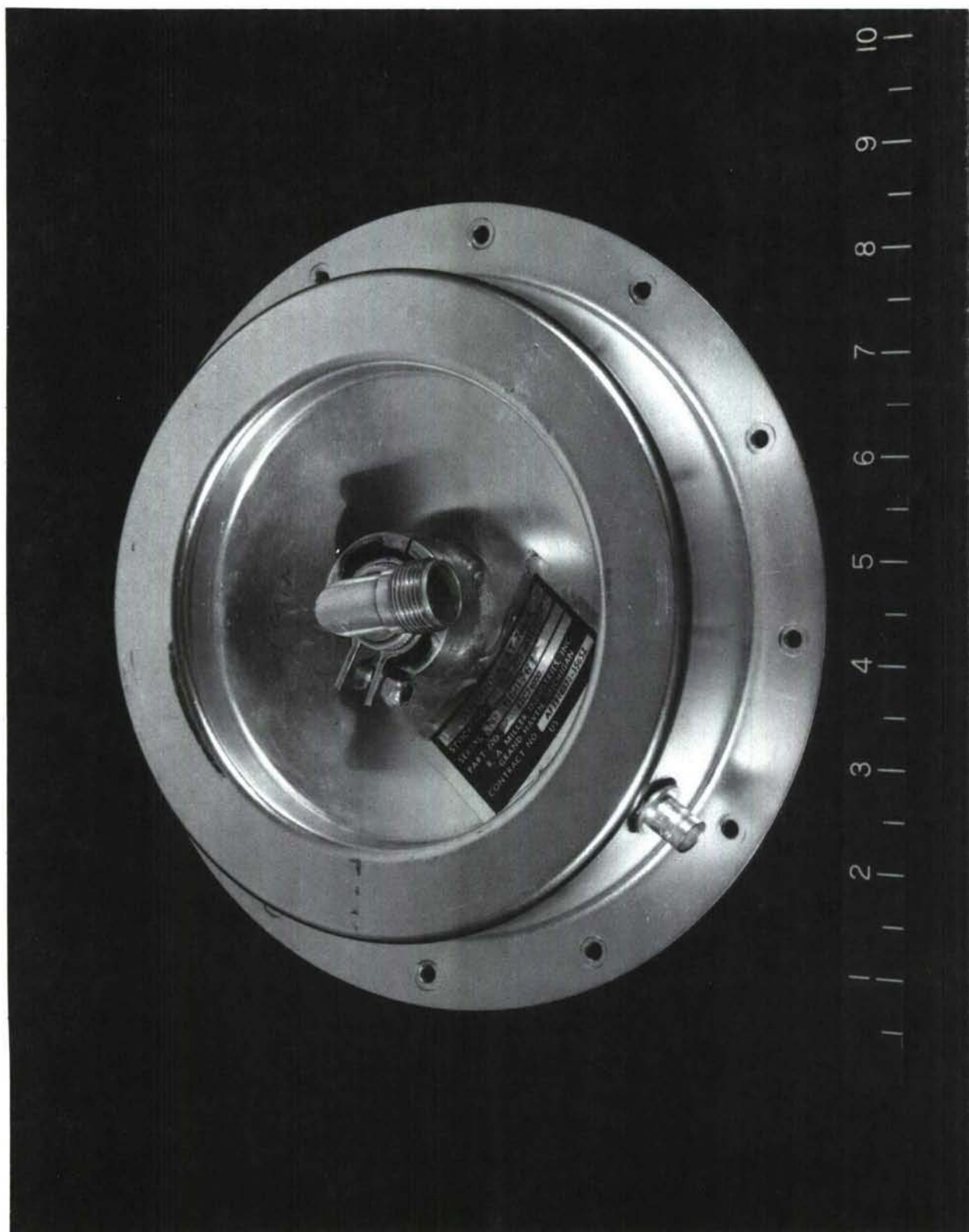


Figure 30. Production Damper Attached to Antenna

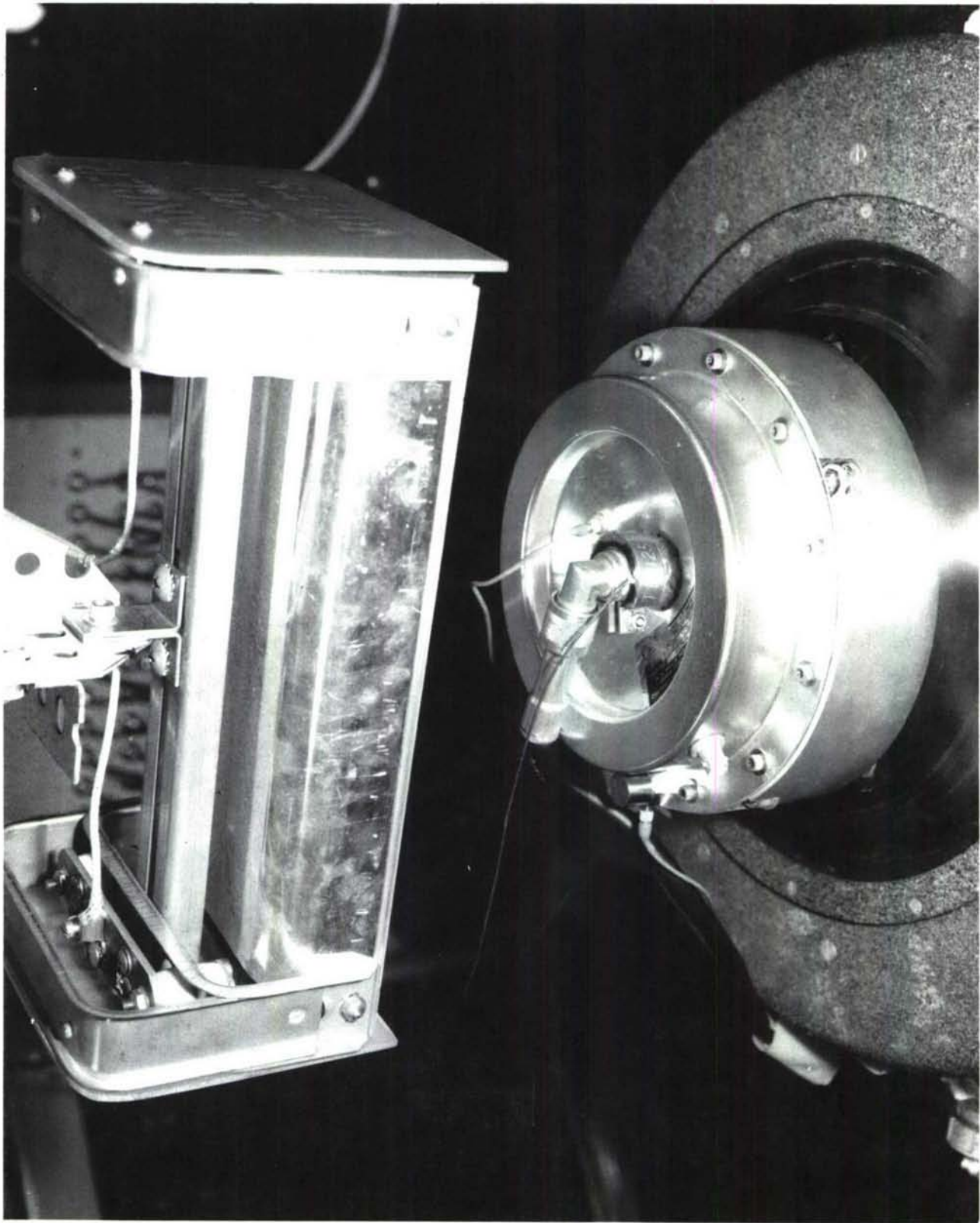


Figure 31. Production Damper Attached to Antenna

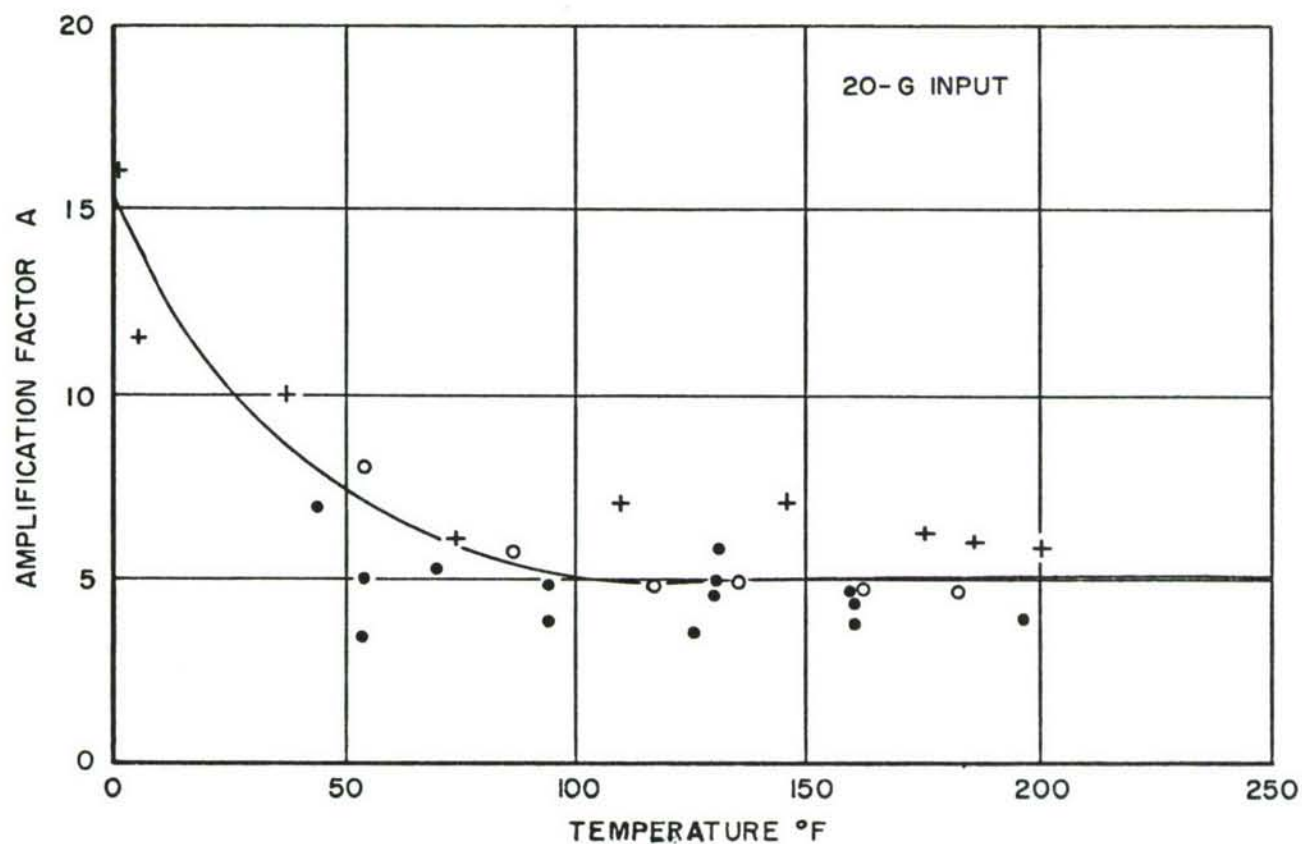
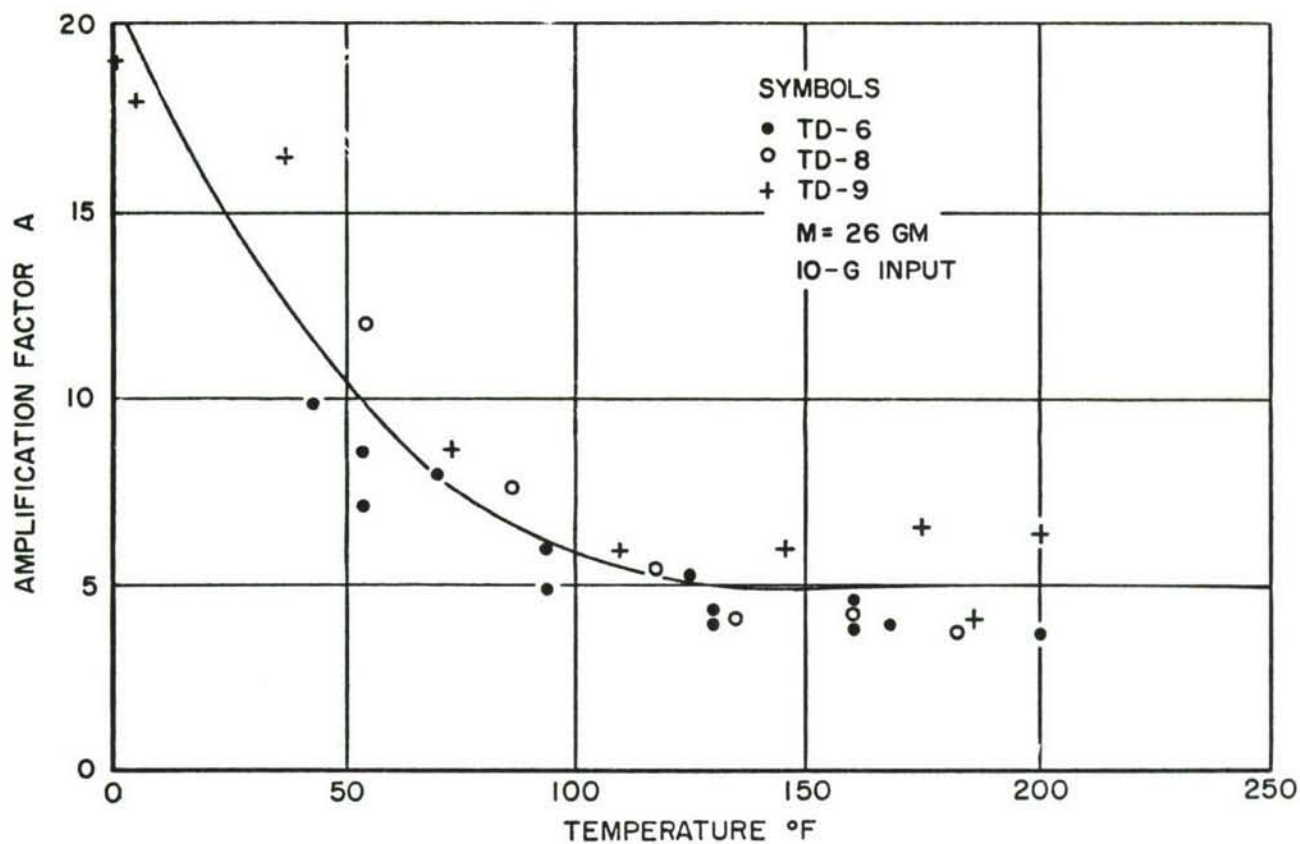


Figure 32. Graphs of Amplification Factor A Against Temperature for Antenna with Prototype 8 Attached

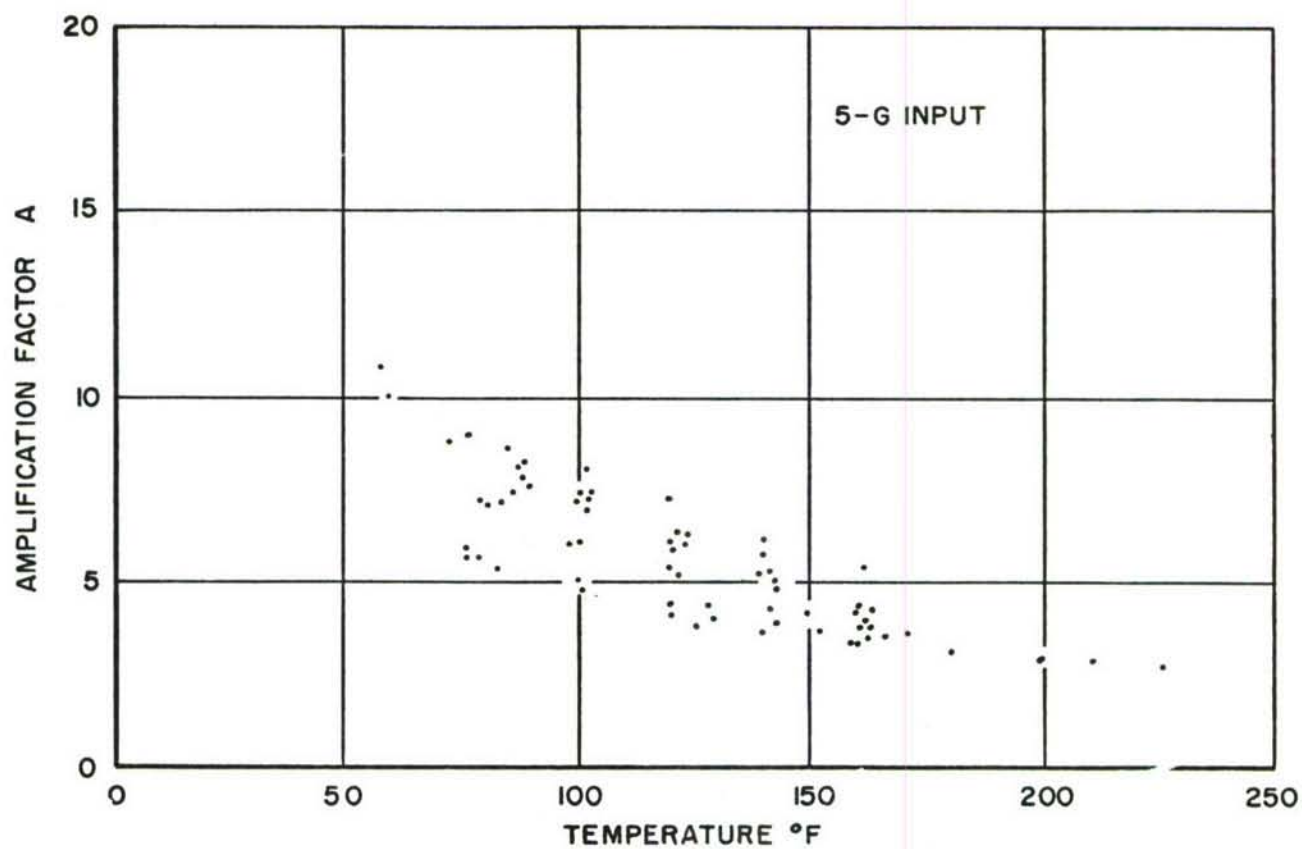
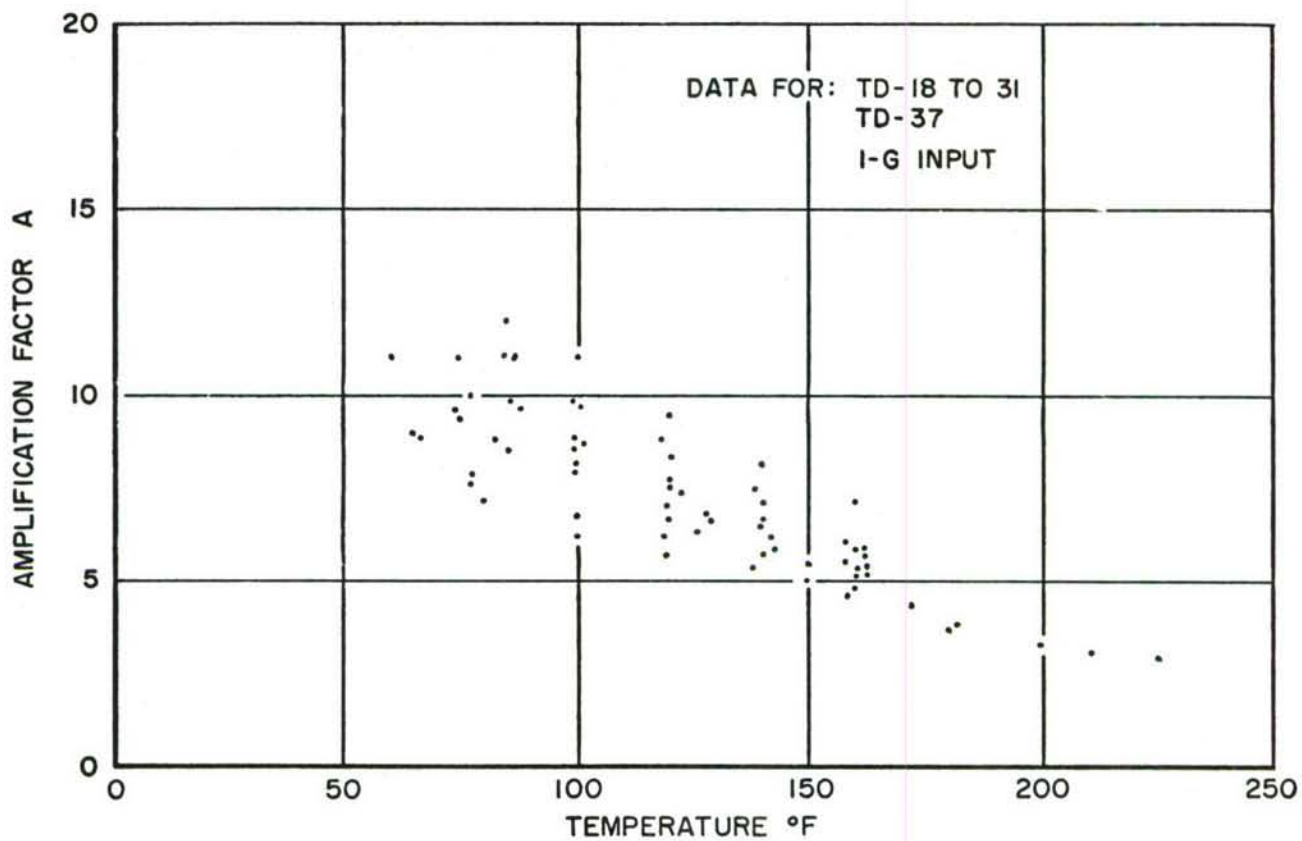


Figure 33. Graphs of Amplification Factor A Against Temperature for Antenna with Production Dampers Attached

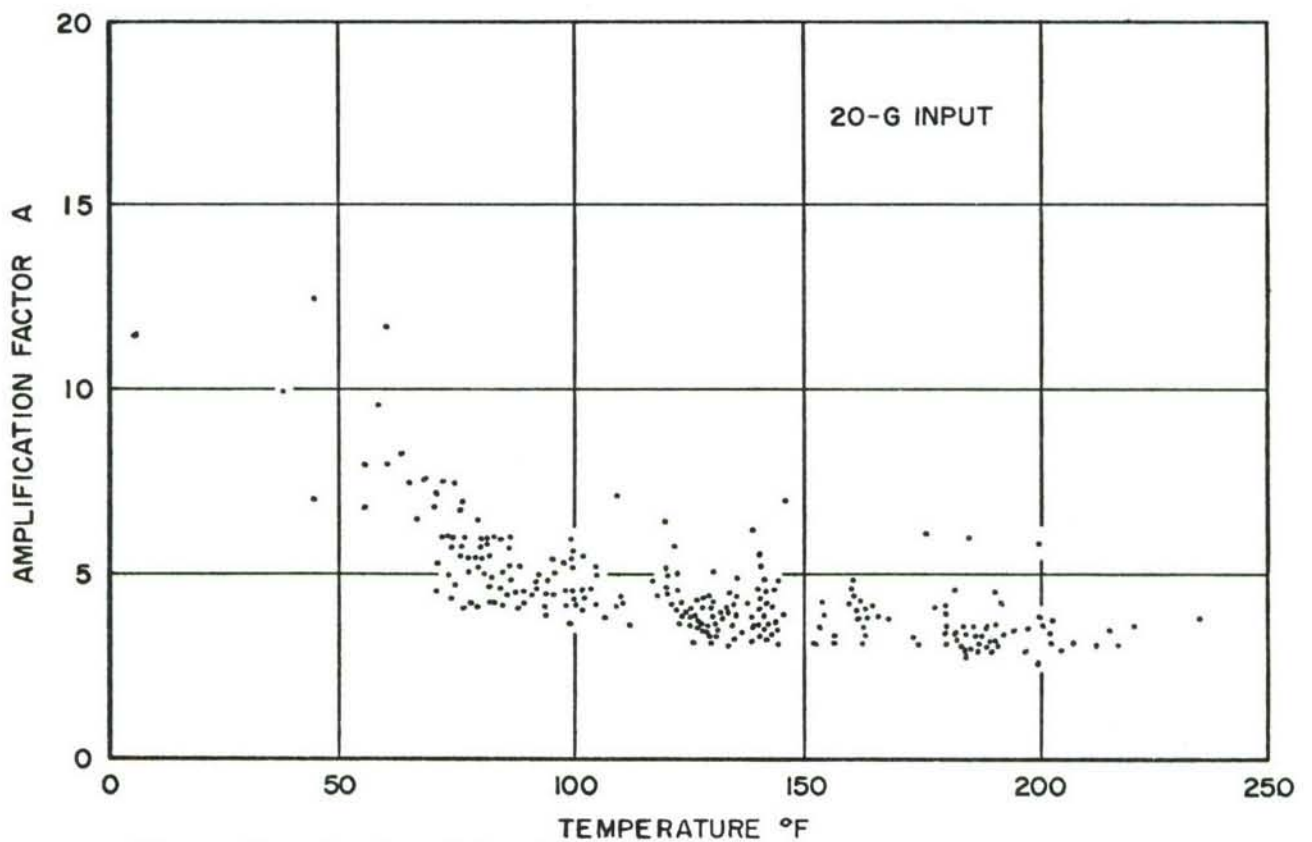
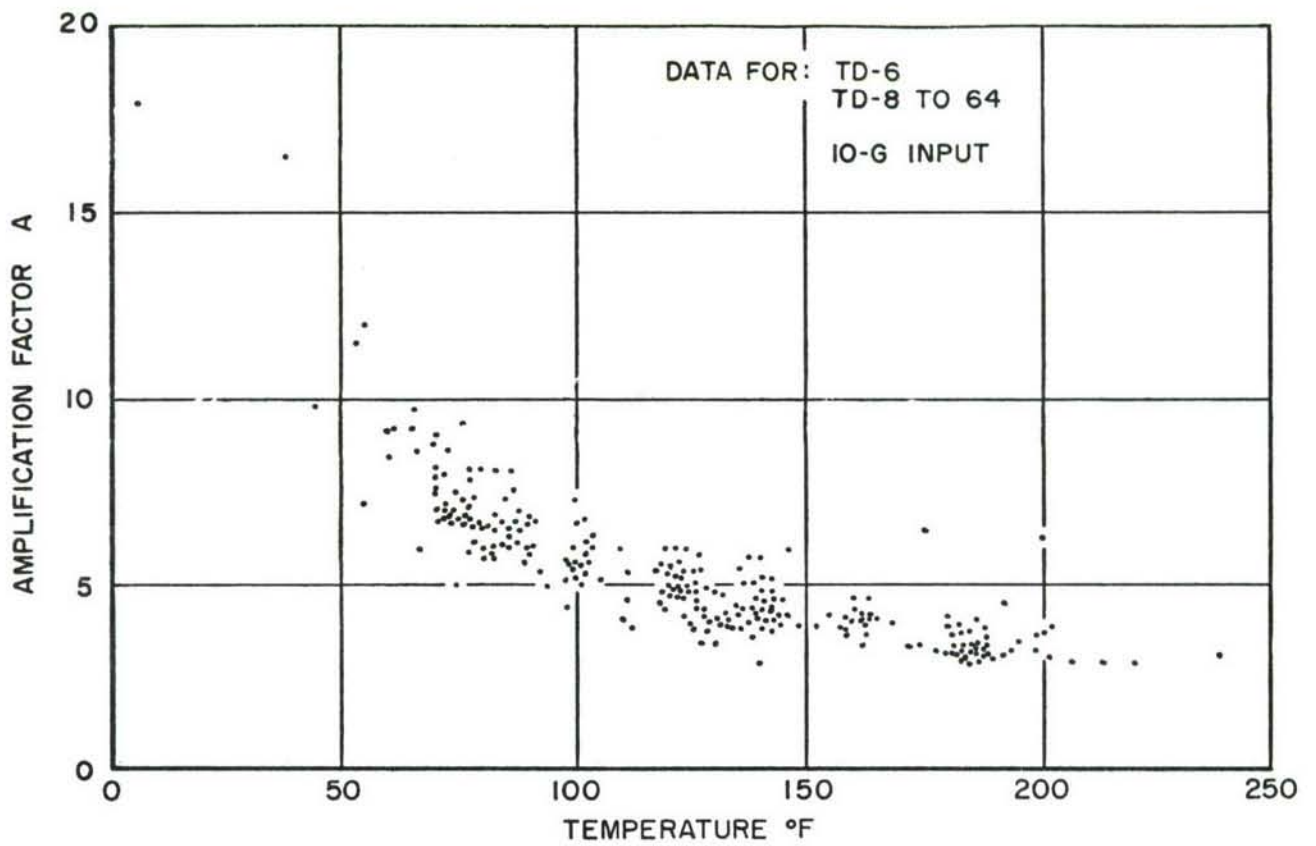


Figure 34. Graphs of Amplification Factor A Against Temperature for Antenna with Production Dampers Attached

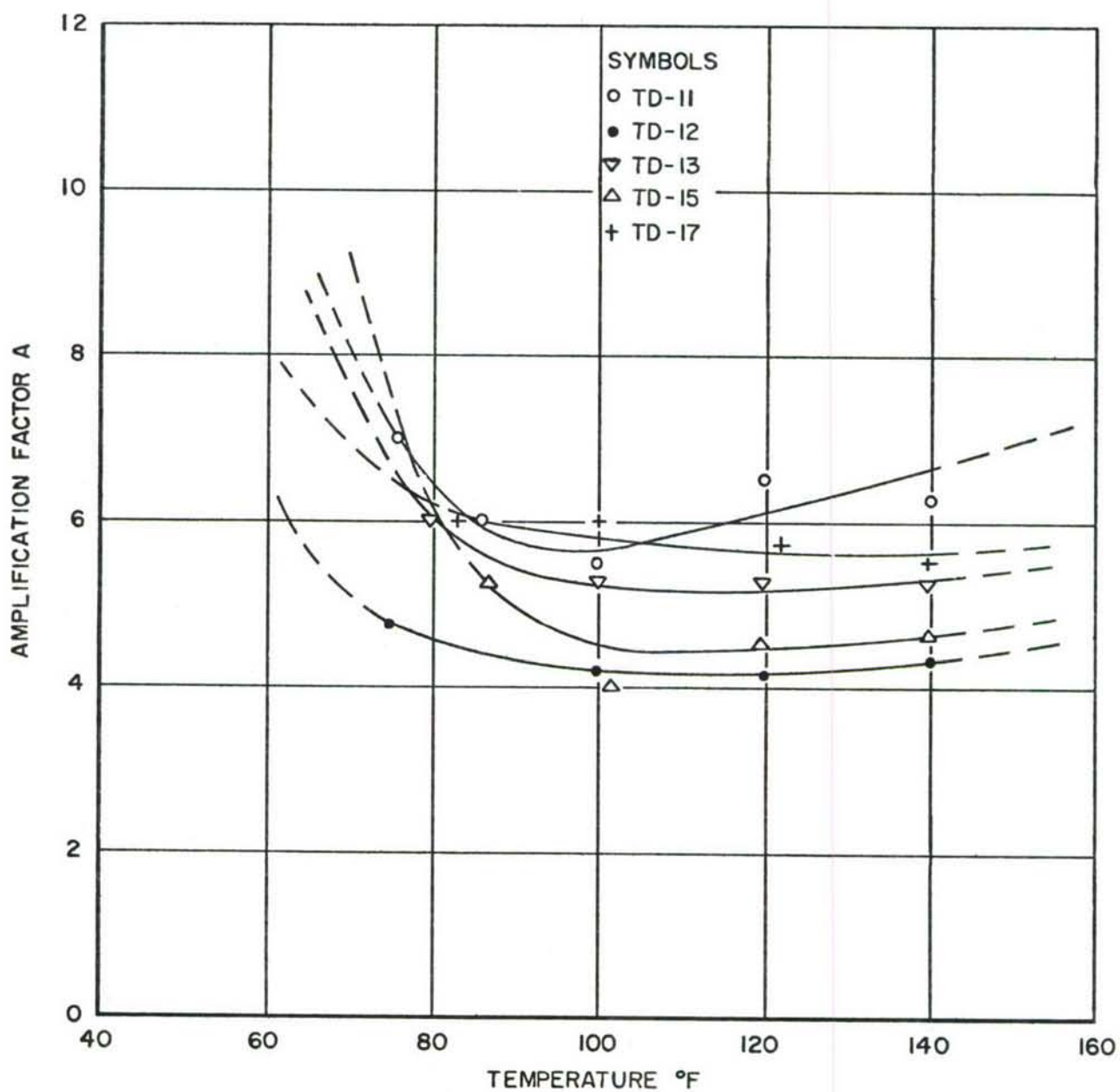


Figure 35. Graph of Amplification Factor A Against Temperature for Antenna with TD-11, 12, 13, 15 and 17 Attached

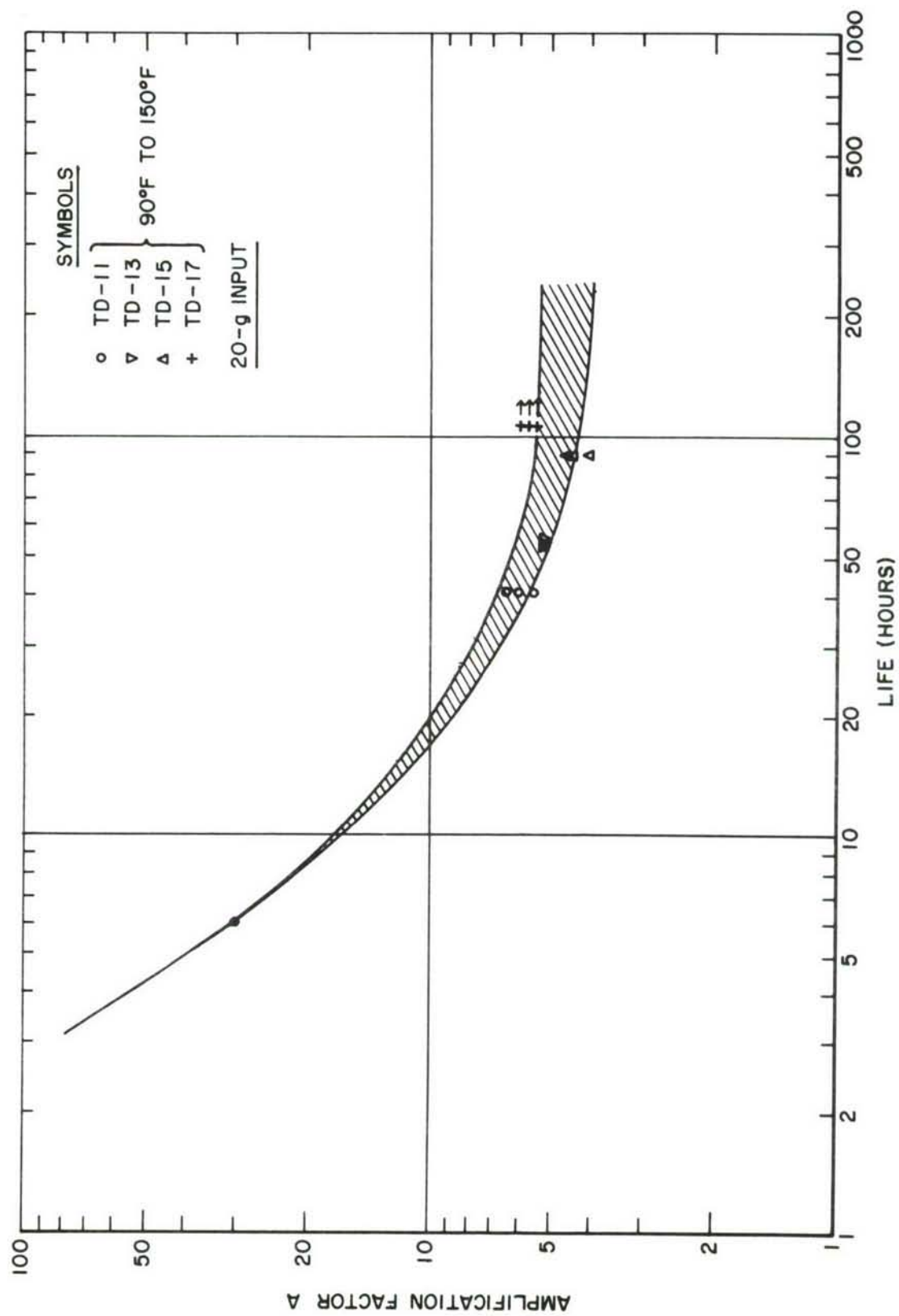


Figure 36. Graph of Amplification Factor A Against Life of Antenna

UNCLASSIFIED

Security Classification

DOCUMENT CONTROL DATA - R&D

(Security classification of title, body of abstract and indexing annotation must be entered when the overall report is classified)

1. ORIGINATING ACTIVITY (Corporate author) Metals and Ceramics Division Air Force Materials Laboratory Wright-Patterson AFB, Ohio 45433		2a. REPORT SECURITY CLASSIFICATION UNCLASSIFIED	
		2b. GROUP	
3. REPORT TITLE DEVELOPMENT OF A TUNED DAMPER TO REDUCE VIBRATION DAMAGE IN AN AIRCRAFT RADAR ANTENNA			
4. DESCRIPTIVE NOTES (Type of report and inclusive dates) January 1966 to May 1967			
5. AUTHOR(S) (Last name, first name, initial) Jones, D.I.G., Nashif, A.D., Bruns, 1/Lt G.H., Sevy, R., Owens, F.S., Henderson, J.P., Conner, R.L.			
6. REPORT DATE September 1967	7a. TOTAL NO. OF PAGES 68	7b. NO. OF REFS 9	
8a. CONTRACT OR GRANT NO. AF 33(615)-1506	9a. ORIGINATOR'S REPORT NUMBER(S)		
b. PROJECT NO. 7351			
c. Task No. 735106	9b. OTHER REPORT NO(S) (Any other numbers that may be assigned this report) AFML-TR-67-307		
d.			
10. AVAILABILITY/LIMITATION NOTICES This document is subject to special export controls and each transmittal to foreign governments and foreign nationals may be made only with the prior approval of the Metals and Ceramics Division, MAM, Air Force Materials Laboratory, Wright-Patterson AFB, Ohio 45433.			
11. SUPPLEMENTARY NOTES		12. SPONSORING MILITARY ACTIVITY Strength and Dynamics Branch Metals and Ceramics Division Air Force Materials Laboratory	
13. ABSTRACT The application of the facilities and expertise of several research and development laboratories at Wright-Patterson Air Force Base, as well as other organizations, to the solution of a critical Air Force vibration problem is described in this technical report. Specifically, the development of a tuned damper to increase the service life of an aircraft radar antenna suffering from severe vibration damage is described. The resulting tuned damper was a wide temperature range device capable of operating satisfactorily in a severe vibrational environment. Criteria necessary for the development of wider temperature range dampers was established in the course of the investigation. This abstract is subject to special export controls and each transmittal to foreign governments and foreign nationals may be made only with the prior approval of the Metals and Ceramics Division, MAM, Air Force Materials Laboratory, Wright-Patterson Air Force Base, Ohio 45433.			

14.	KEY WORDS	LINK A		LINK B		LINK C	
		ROLE	WT	ROLE	WT	ROLE	WT

INSTRUCTIONS

1. **ORIGINATING ACTIVITY:** Enter the name and address of the contractor, subcontractor, grantee, Department of Defense activity or other organization (*corporate author*) issuing the report.

2a. **REPORT SECURITY CLASSIFICATION:** Enter the overall security classification of the report. Indicate whether "Restricted Data" is included. Marking is to be in accordance with appropriate security regulations.

2b. **GROUP:** Automatic downgrading is specified in DoD Directive 5200.10 and Armed Forces Industrial Manual. Enter the group number. Also, when applicable, show that optional markings have been used for Group 3 and Group 4 as authorized.

3. **REPORT TITLE:** Enter the complete report title in all capital letters. Titles in all cases should be unclassified. If a meaningful title cannot be selected without classification, show title classification in all capitals in parenthesis immediately following the title.

4. **DESCRIPTIVE NOTES:** If appropriate, enter the type of report, e.g., interim, progress, summary, annual, or final. Give the inclusive dates when a specific reporting period is covered.

5. **AUTHOR(S):** Enter the name(s) of author(s) as shown on or in the report. Enter last name, first name, middle initial. If military, show rank and branch of service. The name of the principal author is an absolute minimum requirement.

6. **REPORT DATE:** Enter the date of the report as day, month, year, or month, year. If more than one date appears on the report, use date of publication.

7a. **TOTAL NUMBER OF PAGES:** The total page count should follow normal pagination procedures, i.e., enter the number of pages containing information.

7b. **NUMBER OF REFERENCES:** Enter the total number of references cited in the report.

8a. **CONTRACT OR GRANT NUMBER:** If appropriate, enter the applicable number of the contract or grant under which the report was written.

8b, 8c, & 8d. **PROJECT NUMBER:** Enter the appropriate military department identification, such as project number, subproject number, system numbers, task number, etc.

9a. **ORIGINATOR'S REPORT NUMBER(S):** Enter the official report number by which the document will be identified and controlled by the originating activity. This number must be unique to this report.

9b. **OTHER REPORT NUMBER(S):** If the report has been assigned any other report numbers (*either by the originator or by the sponsor*), also enter this number(s).

10. **AVAILABILITY/LIMITATION NOTICES:** Enter any limitations on further dissemination of the report, other than those

imposed by security classification, using standard statements such as:

- (1) "Qualified requesters may obtain copies of this report from DDC."
- (2) "Foreign announcement and dissemination of this report by DDC is not authorized."
- (3) "U. S. Government agencies may obtain copies of this report directly from DDC. Other qualified DDC users shall request through _____."
- (4) "U. S. military agencies may obtain copies of this report directly from DDC. Other qualified users shall request through _____."
- (5) "All distribution of this report is controlled. Qualified DDC users shall request through _____."

If the report has been furnished to the Office of Technical Services, Department of Commerce, for sale to the public, indicate this fact and enter the price, if known.

11. **SUPPLEMENTARY NOTES:** Use for additional explanatory notes.

12. **SPONSORING MILITARY ACTIVITY:** Enter the name of the departmental project office or laboratory sponsoring (*paying for*) the research and development. Include address.

13. **ABSTRACT:** Enter an abstract giving a brief and factual summary of the document indicative of the report, even though it may also appear elsewhere in the body of the technical report. If additional space is required, a continuation sheet shall be attached.

It is highly desirable that the abstract of classified reports be unclassified. Each paragraph of the abstract shall end with an indication of the military security classification of the information in the paragraph, represented as (TS), (S), (C), or (U).

There is no limitation on the length of the abstract. However, the suggested length is from 150 to 225 words.

14. **KEY WORDS:** Key words are technically meaningful terms or short phrases that characterize a report and may be used as index entries for cataloging the report. Key words must be selected so that no security classification is required. Identifiers, such as equipment model designation, trade name, military project code name, geographic location, may be used as key words but will be followed by an indication of technical context. The assignment of links, rules, and weights is optional.